EGG-SEMI-5442

May 1981

POR

QUICK LOOK REPORT FOR SEMISCALE MOD-2A TEST S-UT-7

NRC Research and Technical Assistance Report

R. G. Hanson
D. J. Shimeck
J. L. Steiner

U.S. Department of Energy
Idaho Operations Office • Idaho National Engineering Laboratory

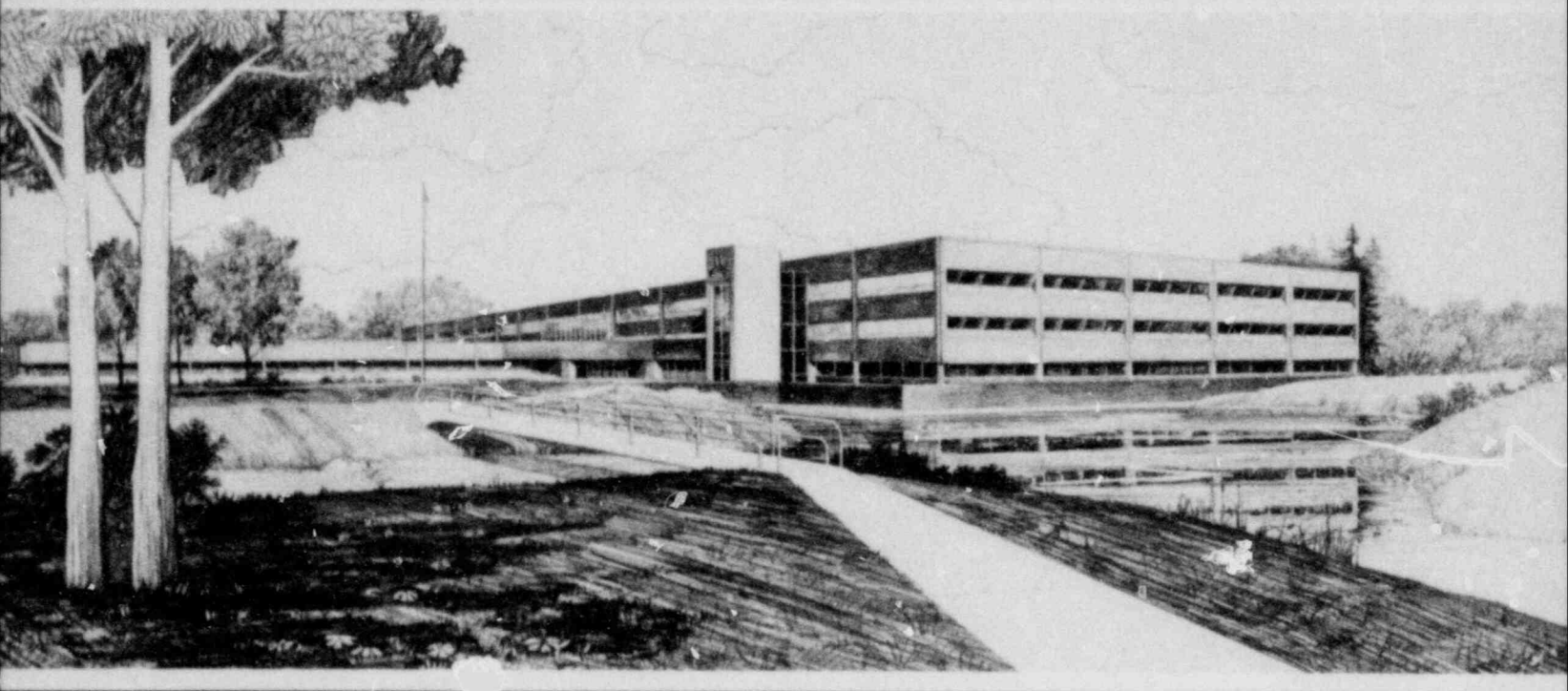

This is an informal report intended for use as a preliminary or working document

Prepared for the
U.S. Nuclear Regulatory Commission
under DOE Contract No. DE-AC07-761D01570
FIN No. A6038

EG&G Idaho

EG&G Idaho, Inc.

FORM EG&G-398
(Rev. 05-79)

INTERIM REPORT

Accession No. _____

Report No. EGG-SEMI-5442

Contract Program or Project Title:

Water Reactor Research Test Facilities Division

Subject of this Document:

Quick Look Report for Semiscale
Mod-2A Test S-UT-7

Type of Document:

Quick Look Report

Author(s): R. G. Hanson
D. J. Shimeck
J. L. Steiner

Date of Document:

May 13, 1981

Responsible NRC Individual and NRC Office or Division:

W. C. Lyon, Reactor Safety Research

EG&G Idaho, Inc.
Idaho Falls, Idaho 83401

Prepared for the
U.S. Nuclear Regulatory Commission
Washington, D.C.
Under DOE Contract No. DE-AC07-76ID01570
NRC FIN No. A6038

INTERIM REPORT

QUICK LOOK REPORT FOR
SEMISCALE MOD-2A
TEST S-UT-7

by

R. G. Hanson
D. J. Shimeck
J. L. Steiner

Approval: _____

G. W. Johnsen, Manager
WRRTF Experiment Planning
and Analysis Branch

Approval: _____

P. North, Manager
Water Reactor Research
Test Facilities

CONTENTS

FIGURES

TABLES

ABSTRACT

Results are presented from a preliminary analysis of Semiscale Mod-2A Test S-UT-7. This test simulated a 5%, communicative break in the cold leg of a pressurized water reactor equipped with upper head emergency core coolant injection (UHI) capability. Initial conditions were typical of, or scaled from, a UHI plant. The primary objective of the test was to investigate the distribution of UHI water, and its influence on transient behavior, through comparison with Semiscale Mod-2A Test S-UT-6 which was similar but did not use UHI.

SUMMARY

This report presents the results of a preliminary analysis of data from Semiscale Mod-2A small break Test S-UT-7. This test simulated a loss-of-coolant accident resulting from a 5% communicative break in the cold leg of a pressurized water reactor (PWR). The break size for this test was 0.1123 cm^2 which is volumetrically scaled to represent a 15.6 cm diameter pipe break in a PWR. The Mod-2A system was configured to simulate a PWR with the capability to inject emergency core coolant (ECC) into the vessel upper head. The upper head accumulator was pressurized to 8.6 MPa and the loop accumulator pressures were set at 2.86 MPa, as is nominally specified for upper head injection (UHI) plants. Data from a previous test (S-UT-6) was used to establish the baseline response of the Mod-2A system for a 5% break without UHI for similar test conditions. Comparison of system responses between Tests S-UT-6 and S-UT-7 allowed an evaluation of the influence of UHI.

Initial conditions for the test were equivalent to, or scaled from, typical PWR operating conditions. Following rupture of the pressure boundary, continuous depressurization took place and the system was observed to void predominantly from the upper elevations downward. The injection of UHI liquid into the vessel upper head caused a delayed and slower draining of the head. It also caused a more rapid depressurization during the period of injection than was observed in Test S-UT-6. As the system voided, fluid in the pump suctions formed a seal which impeded steam flow around the loops. The formation of the suction seals depressed the liquid level in the core but did not result in any dryouts of the heater rods. Once the intact loop pump suction had cleared the cold leg emptied, uncovering the break. The liquid remaining in the vessel then slowly boiled off until the system depressurized to the loop accumulator pressure of 2.86 MPa at 738 s. Some dryouts were observed in the upper part of the core beginning at 680 s. Dryouts only occurred at about the top 60 cm of the core and rewetting occurred rapidly once loop accumulator injection began. The rod temperatures at initial conditions were the highest

observed for the entire experiment. Measurements indicate that much of the UHI liquid exited the upper head through the bypass line to the downcomer and cold legs and subsequently flowed out the break by 300 s. However, enough UHI liquid flowed into the core and downcomer to keep the minimum core liquid level to 160 cm versus a minimum of 115 cm which occurred in Test S-UT-6.

Results of the RELAP5 pretest prediction generally compared well with test data. The first 200 s of the transient was predicted well with respect to system depressurization, core temperatures, and upper head drainage. The code calculated vapor velocity at the break was too high after 200 s. As a result, the calculated system pressure and core collapsed liquid level were lower than data indicated. Posttest analysis improvements to the RELAP5 calculations will investigate the representation of slip at the break and its effect on system depressurization and vapor generation in the vessel.

1. INTRODUCTION

Testing performed in the Semiscale Mod-2A system is part of the water reactor safety research effort directed toward assessing and improving the analytical capability of computer codes which are used to predict the behavior of pressurized water reactors (PWR's) during postulated accident scenarios. For this purpose, the Mod-2A system was designed as a small-scale model of the primary system of a four-loop PWR nuclear generating plant. The system incorporates the major components of a PWR including steam generators, vessel, pumps, pressurizer, and loop piping. One loop (intact loop) is scaled to simulate the three intact loops in a PWR, while the other (broken loop) simulates the single loop in which a break is postulated to occur in a PWR. Geometric similarity has been maintained between a PWR and Mod-2A, most notably in the design of a 25 rod, full-length (3.66 m), electrically heated core, full-length upper head and upper plenum, component layout, and relative elevations of various components. Equipment in the upper head of the Mod-2A vessel has been designed to simulate the fluid flow paths found in a PWR which has the capability of injecting emergency core coolant (ECC) into the upper head. The scaling philosophy followed in the design of the Mod-2A system (modified volume scaling) preserves most of the important first-order effects thought important for small break loss-of-coolant transients.[1]

This report presents a preliminary analysis of data from Semiscale Test S-UT-7, the seventh and final test conducted in the UT test series. The primary objective of the UT test series is to evaluate the capability of the upper head injection (UHI) system to provide an increased margin against core uncovery in the Semiscale system during small break transients. The test series investigated transients for 2-1/2%, 5%, and 10% cold leg breaks. For each break size a test was first conducted which did not use UHI but did employ loop accumulators pressurized to 2.86 MPa to establish baseline response data. These were followed by similar tests which used the UHI system in addition to loop accumulator injection. Tests results will provide applicable data for use in the assessment of computer codes used to predict the behavior of UHI systems.

Test S-UT-7 was a 5%, communicative, cold leg break loss-of-coolant experiment performed with upper head accumulator injection. This test provided information on the influence of upper head injection on system transient response which will be evaluated by comparison to a counterpart test (S-UT-6)[2]; a 5% break experiment without ECC injected into the upper head.

The following sections present a preliminary analysis of Test S-UT-7. Section 2 describes the system hardware, test procedures, and initial conditions. Section 3 presents the results of the test data analysis including a comparison to Test S-UT-6. Section 4 compares the actual system response with the computer code pretest prediction and Section 5 presents conclusions drawn from a preliminary analysis of the data.

2. SYSTEM CONFIGURATION AND TEST CONDUCT

2.1 System Configuration

An isometric of the Semiscale Mod-2A system, as configured for Test S-UT-7, is shown in Figure 1 with major components identified. The break was located in the broken loop cold leg between the pump and the vessel and was communicative in nature. The break assembly and orifice are shown in detail in Figure 2. The break size was 0.1123 cm^2, which is volumetrically scaled to represent 5% of the cross sectional area of a cold leg pipe in a PWR. The orifice was designed as bell-mouthed with a length-to-diameter ratio of approximately three.

Figure 3 is a plan view of the Mod-2A core for Test S-UT-7 showing its orientation with respect to the remainder of the system, the location of unpowered rods, and the distribution of internal cladding thermocouples monitored during the test. Internally heated electric rods are used to simulate the nuclear rods in a PWR. The rods are geometrically similar to nuclear rods with a heated length of 3.66 m and an outside diameter of 1.072 cm. The axial power profile for the rods is illustrated in Figure 4, showing the step cosine shape with a 1.55 peak-to-average power factor. All 23 heated rods were powered equally. The total core power was 2.0 MW which yielded a maximum linear heat generation rate of 36.85 kW/m. The relative locations of in-core instrumentation (gamma densitometers and core inlet drag screen) and grid spacers are shown in Figure 5.

Figure 6 shows the configuration of the upper head region of the Mod-2A vessel. The internals of the upper head have been designed to simulate the flow paths found in a PWR with UHI capability. Penetrations into the upper head consist of a perforated ECC injection tube, a bypass line from the top of the downcomer, a simulated control rod guide tube, and two simulated support columns.

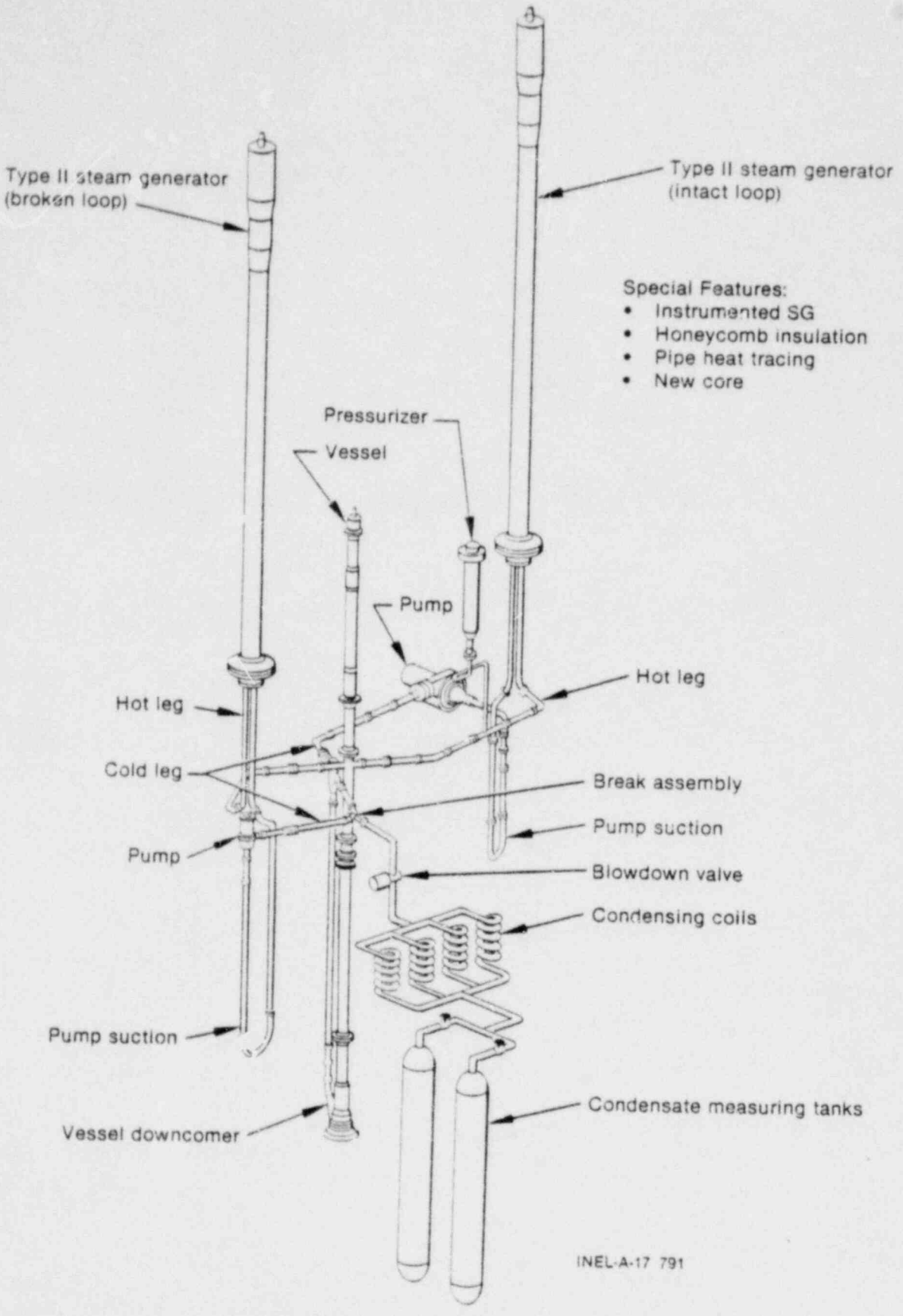

Figure 1. Semiscale Mod-2A system as configured for Test S-UT-7.

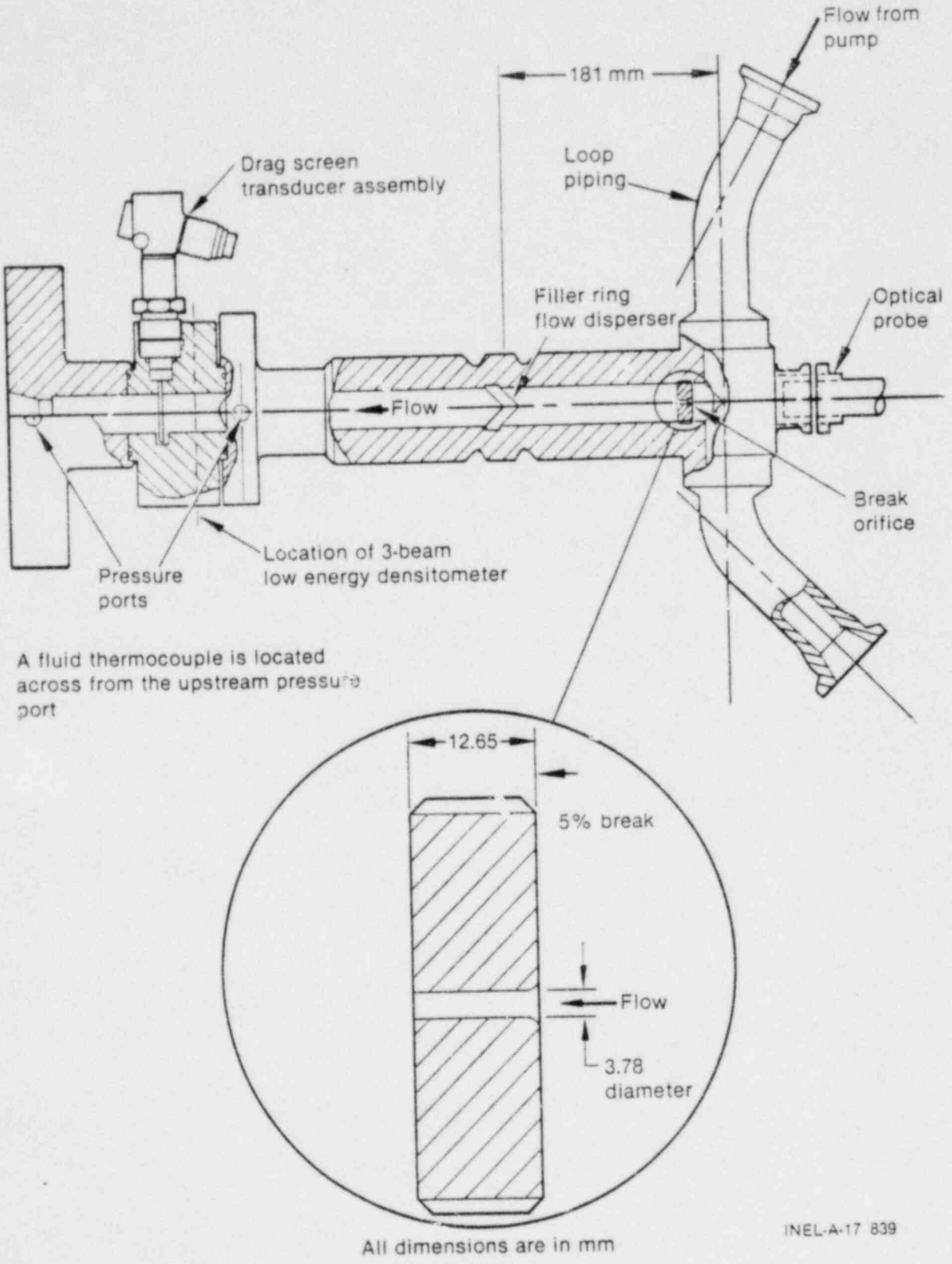

Figure 2. Communicative break assembly and orifice for a 5% break.

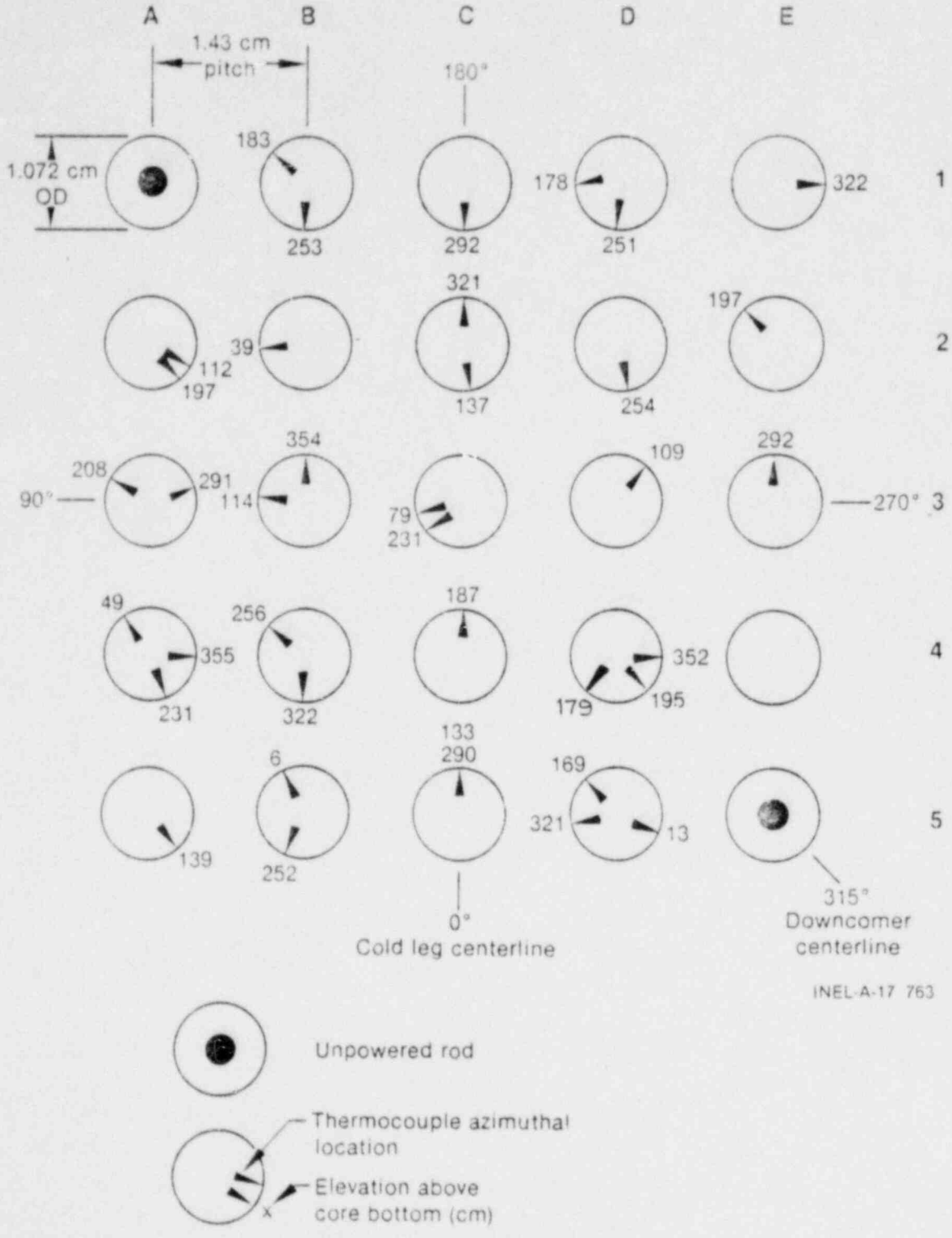

Figure 3. Plan view of the Mod-2A core showing heater rod thermocouple locations for Test S-UT-7.

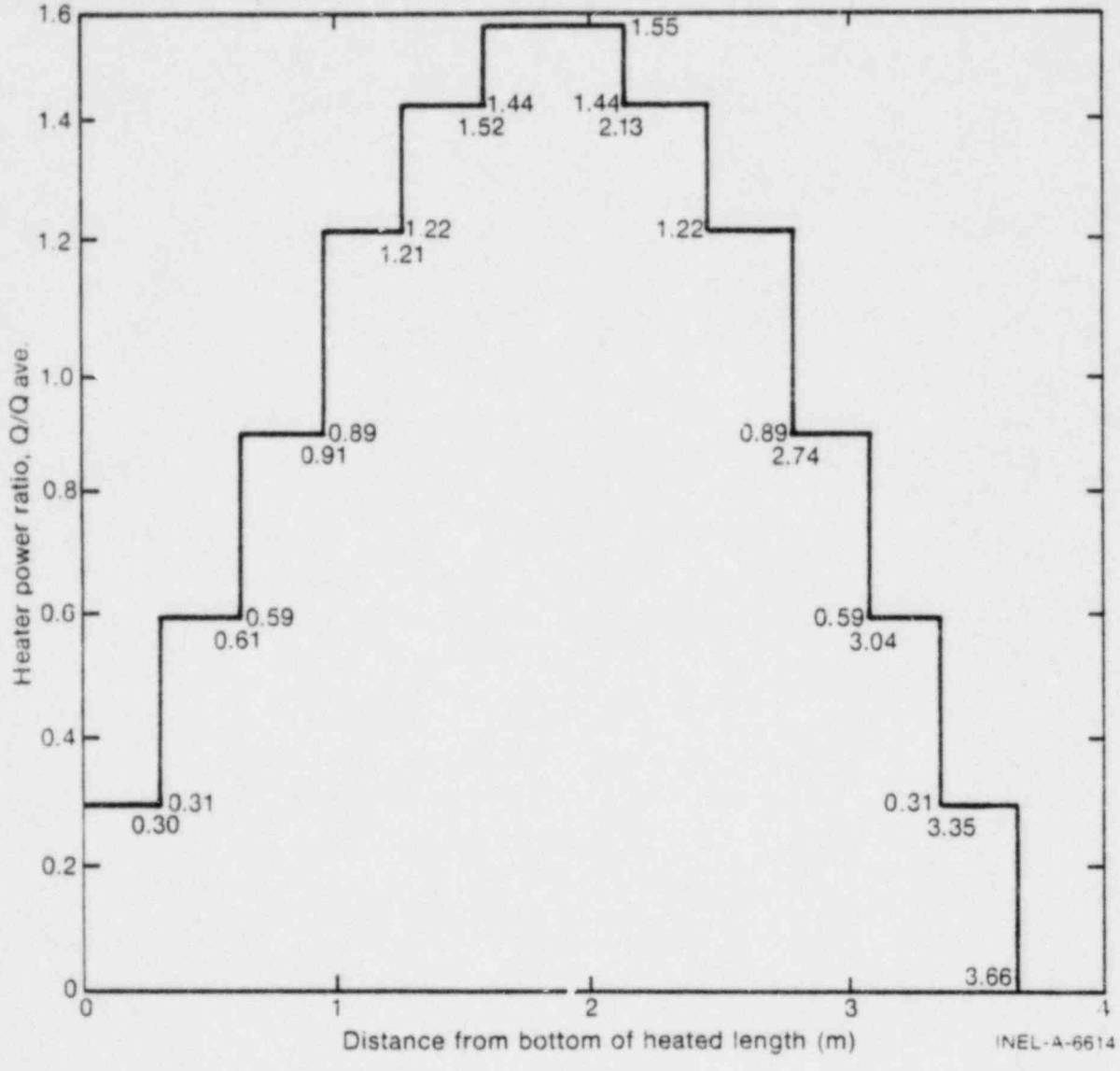

Figure 4. Semiscale Mod-2A heater rod axial power distribution.

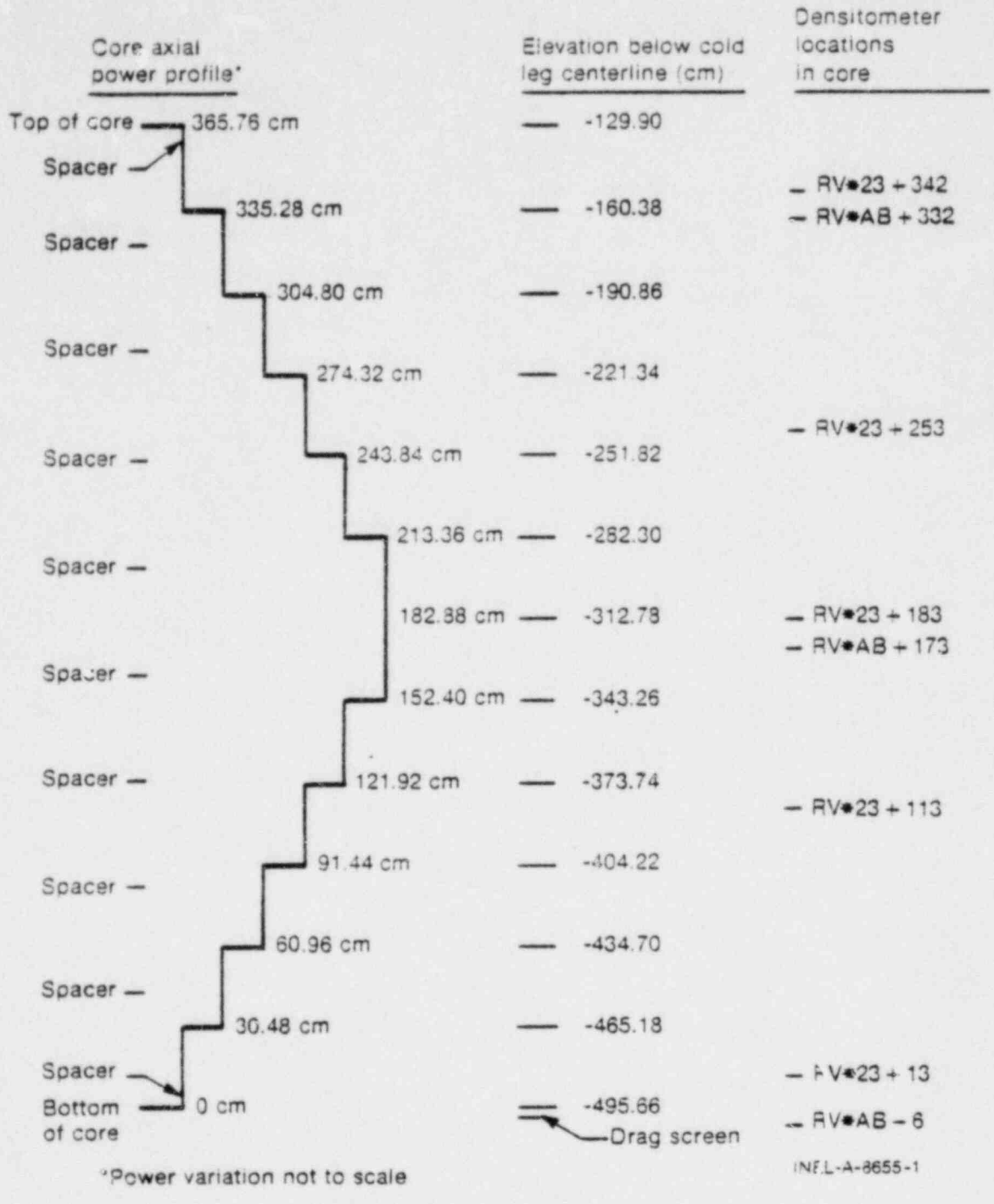

Figure 5. Core axial power profile and vessel instrumentation locations.

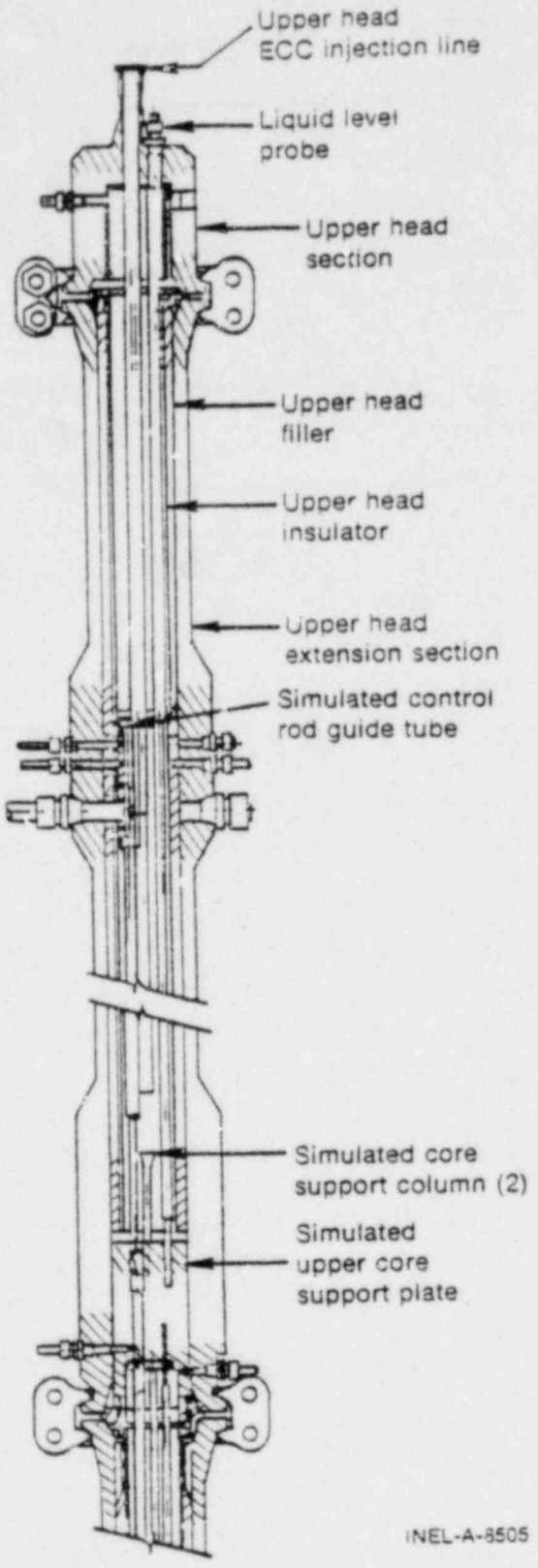

Figure 6. Upper head geometry for the Semiscale Mod-2A vessel.

The heat loss makeup system for the Mod-2A facility is composed of numerous heater bands and tapes on the loop piping and five variable power supplies. Heater bands and tape were installed on the piping where space allowed. The heaters are controlled in five power banks; intact loop hot leg, intact loop cold leg, intact loop pump suction, broken loop hot and cold leg, and broken loop pump suction. The total operating capacity of the system is approximately 51 kW. A more detailed description of the system may be found in Reference 3. A representation of the distribution of heaters may be seen in the computer code system model in the appendix.

The data acquisition system recorded measurements from approximately 275 instruments throughout the system. These measurements included fluid and metal temperatures, pressures, fluid densities, flow rates, liquid levels, and other system parameters. A more detailed description of the Mod-2A system may be found in Reference 3.

2.2 Test Procedures and Conditions

2.2.1 Preblowdown Activities

Prior to the initiation of the test, the Semiscale system was filled with demineralized water and vented to ensure a liquid-full system. Water in the steam generator feedwater tank was heated to the desired temperature. Accumulator water levels were established and the accumulators were pressurized with nitrogen gas to the desired pressure. The accumulators used in this test injected water into the upper head and the intact and broken loop cold legs. Instrumentation was calibrated and zeroed as necessary and a system hydrostatic test was performed.[a] After the necessary protective trip controls and peripherial hardware controls (pumps, valves, etc.) had been set, the system was brought to initial

---

a. The measured leak rate for Test S-UT-7 was 0.0114 ℓ/s at initial conditions. This is much smaller than the break flow rate during the early portion of the transient. The leak rate generally decreases with system pressure and with increased system voiding.

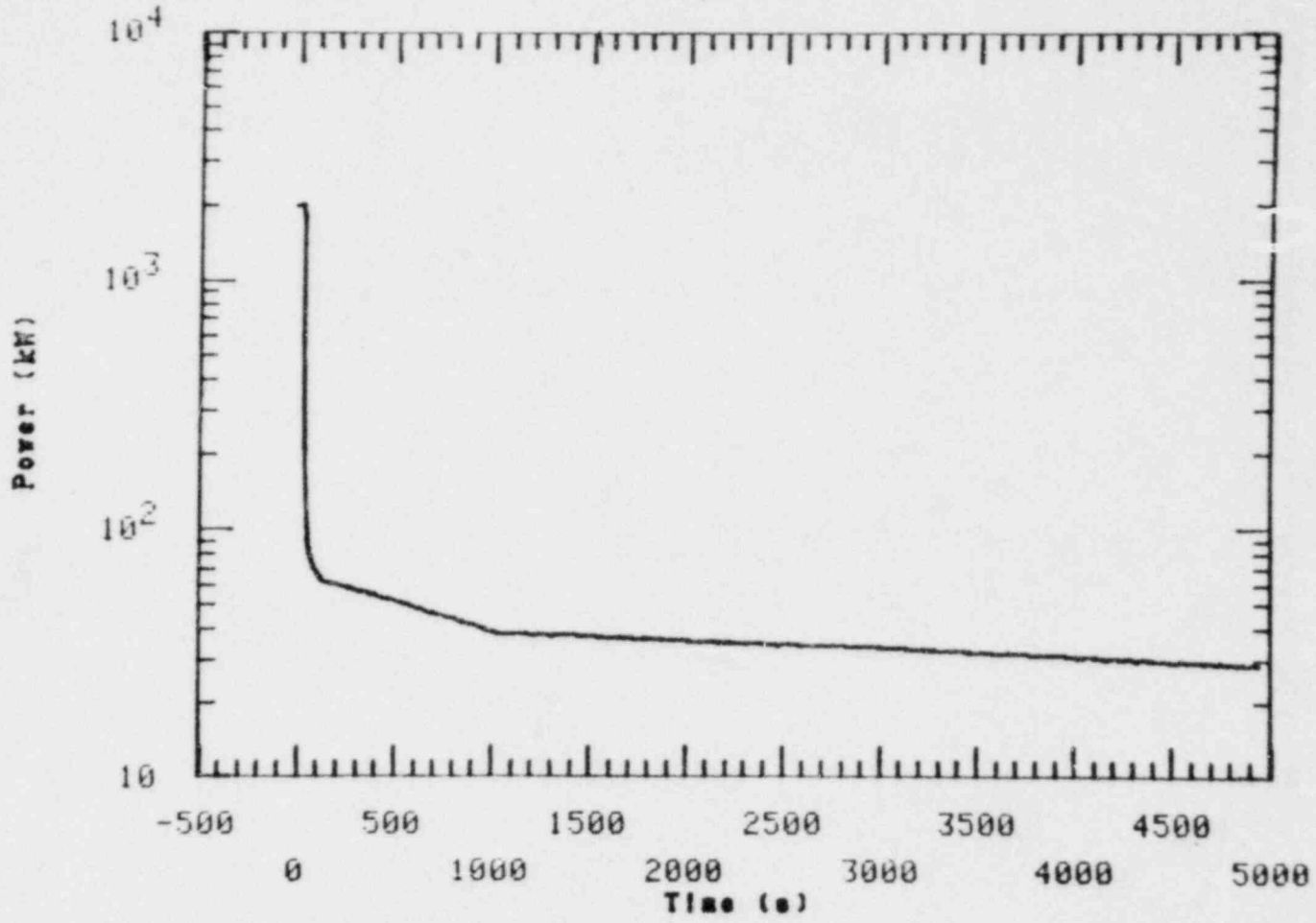

Figure 7. Core power for Test S-UT-7.

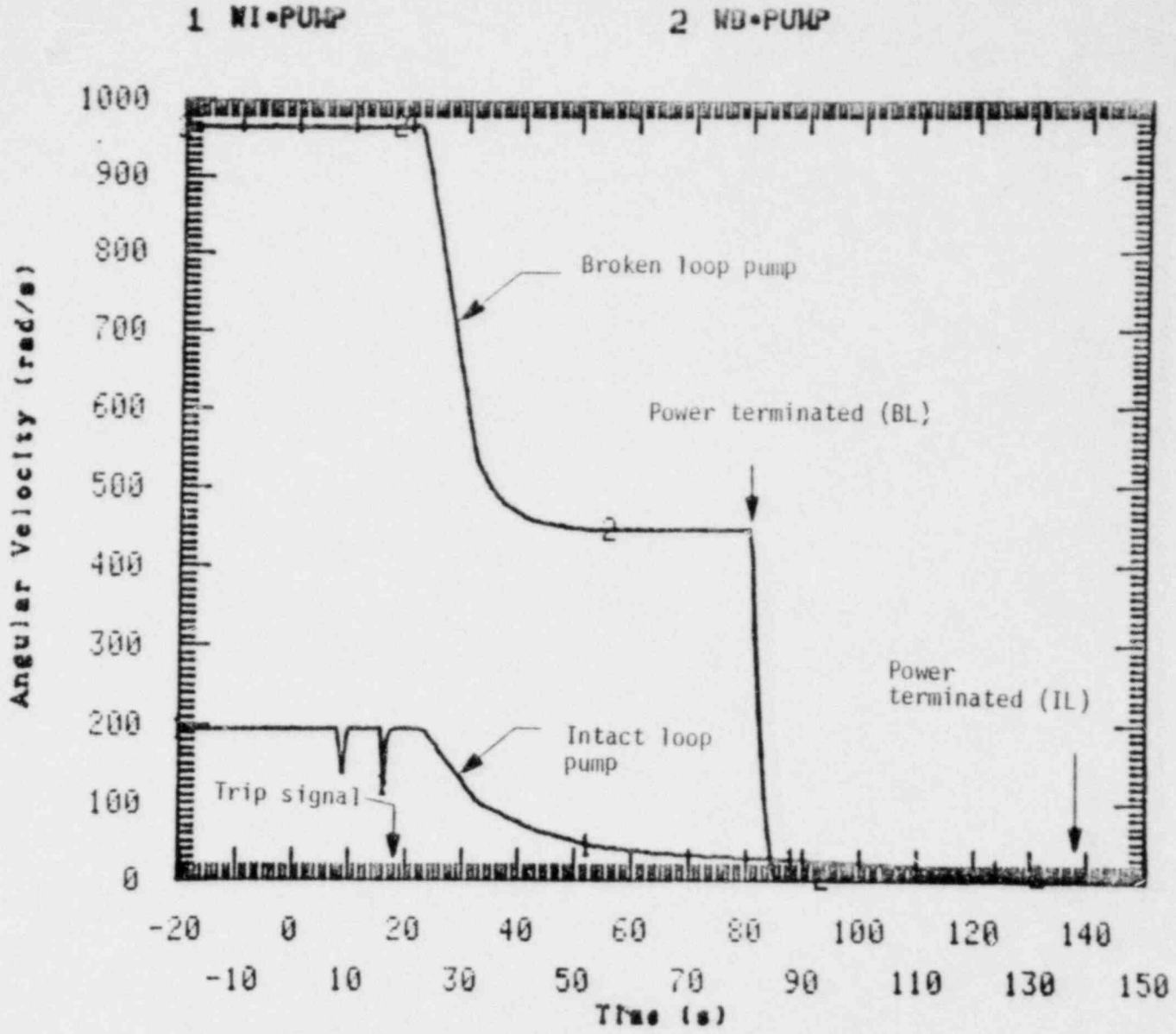

Figure 8. Intact and broken loop pump speed curves for Test S-UT-7.

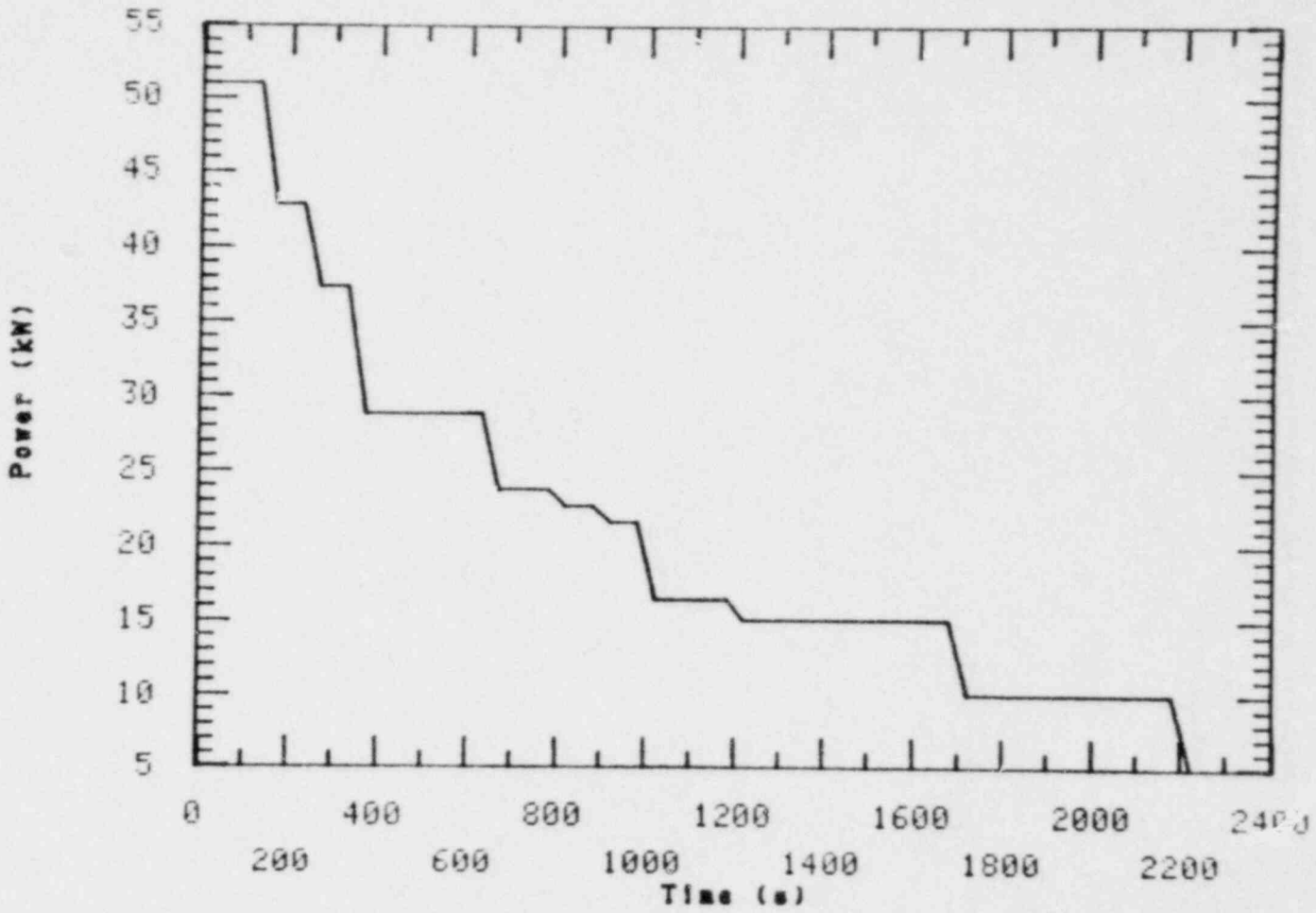

Figure 9. Loop piping heater power for Test S-UT-7.

conditions and the required levels were established in the steam generator secondary sides. Power for the external heaters on the loops was brought to specified conditions and the system was allowed to equilibrate.

When initial conditions were within specified tolerances, the test was initiated by opening a blowdown valve downstream of the break orifice to break the system pressure boundary.

2.2.3 Component Controls

Transient core power control and the intact and broken loop pump speed controllers were initiated by a pressure trip 2.4 s after the pressurizer pressure reached 12.9 MPa. Both intact and broken loop steam generator steam valves were sequenced to close when the pressure trip occurred. Both steam generator feedwater valves were sequenced to close 24 s later.[a] The core power curve and pump speed curves are shown in Figures 7 and 8 respectively. More discussion of how the core electric power curve was determined, and how other various component controls were selected, may be found in Reference 4.

The heaters on the intact and broken loop piping were controlled to offset system heat losses to the extent possible. The power to the heaters was determined by analysis of pretest scoping calculations which compared Mod-2A response for various control schemes against an ideal system with no heat losses. Heater band power was controlled on-line according to the data presented in Figure 9. The heaters are initially powered at 51 kW which is approximately the maximum system operating limit. Power was decreased as the transient proceeded in response to the predicted voiding of the loops and resultant decreased fluid to pipe heat transfer.

The HPIS and LPIS injection rates were controlled on a flow rate versus system pressure basis to simulate the characteristics of a PWR

---

a. The Mod-2A steam generators operate with a lower than desired secondary liquid level at initial conditions. Extra feedwater is injected for 24 s to ensure that the tubes are covered for the transient.

plant. The specification for pumped injection assumes one of two ECC and charging pump trains fail resulting in only 78% of the flow from two train operation. The HPIS flow for the broken loop was mistakenly deleted as described in the next section. The actual intact and broken loop HPIS and LPIS flow rates versus pressure for the test are shown in Figure 10. The LPIS injection rate for the intact loop is simply added to the HPIS flow rate for pressures below 0.98 MPa.

2.2.3 Initial Conditions and ECC Parameters

The specified and actual test conditions for Test S-UT-7 are compared in Table 1. In general, the initial conditions and test parameters were judged as satisfactory to meet the test objectives. One notable difference was the failure to inject HPIS ECC water into the broken loop cold leg. However, the amount of HPIS injected into the broken loop is small. The expected effect of the failure to inject was deemed minimal since no significant core dryout was observed even without the broken loop HPIS. The experiment was therefore considered acceptable for addressing the objectives of evaluating the influence of UHI.

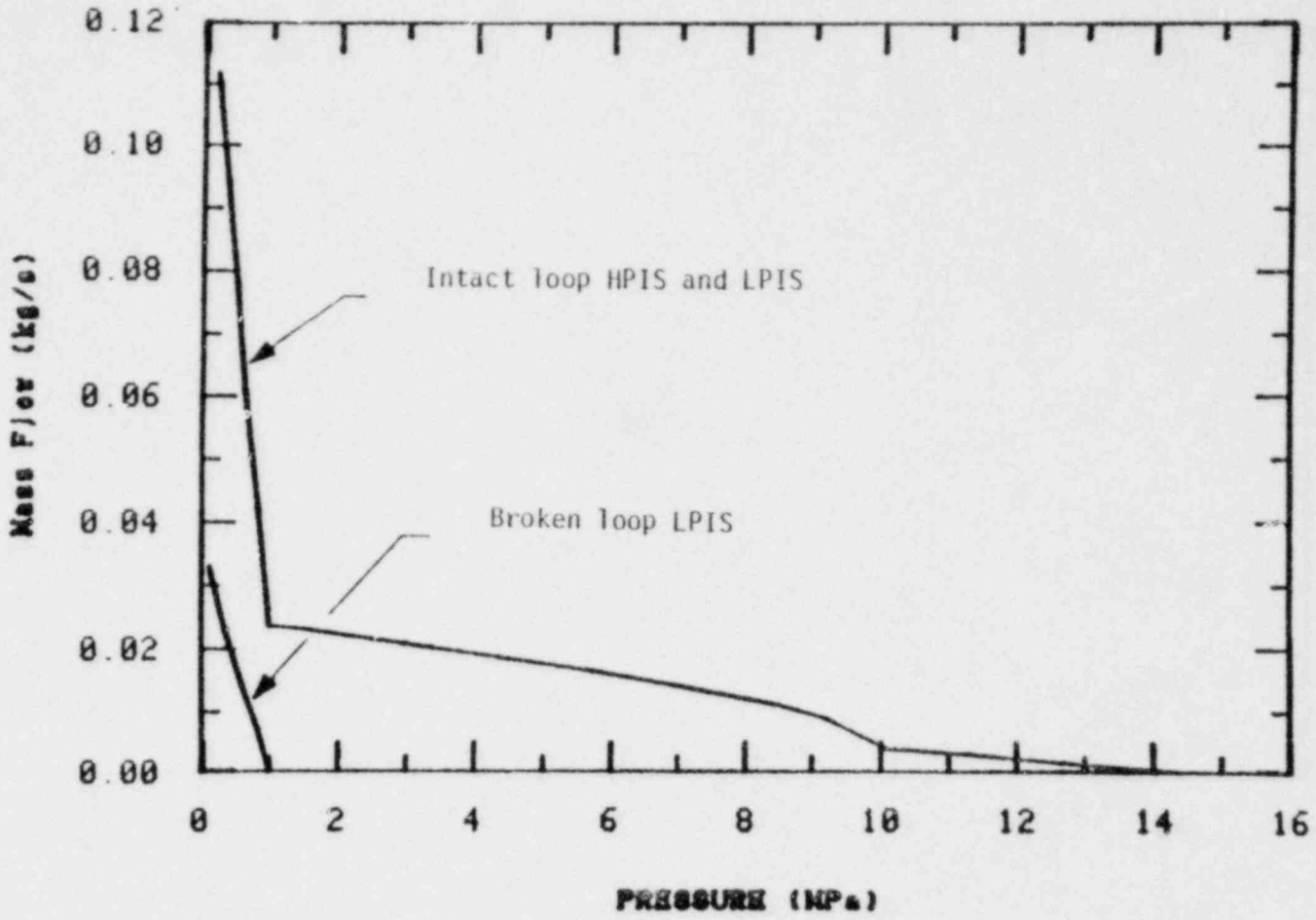

Figure 10. High and low pressure ECC injection system control for intact and broken loops.

TABLE 1. INITIAL CONDITIONS AND ECC REQUIREMENTS FOR TEST S-UT-7

Parameter	Specified Value	Actual Value
Initial Conditions		
Pressurizer pressure	15.5 ± 0.2 MPa	15.5 MPa
Hot leg fluid temperature	594 ± 2 K	598 K
Cold leg fluid temperature	557 ± 2 K	558 K
Total core power	2.0 ± 0.005 MW	2.0 MW
Radial power profile	Flat	
Core inlet flow rate	9.77 kg/s[a]	9.0 kg/s
Pressurizer liquid mass	10.4 ± 0.1 kg	10 [c] kg[d]
S.G. secondary pressure		
Intact loop	5.9 ± 0.2 MPa[b]	5.7 MPa
Broken loop	5.9 ± 0.2 MPa[b]	5.92 MPa
S.G. feedwater temperature		
Intact loop	495 ± 2 K	502 K
Broken loop	495 ± 2 K	497
S.G. secondary water level		
Intact loop	Footnote b	1112 cm[e]
Broken loop	Footnote b	1000 cm[e]
Configuration		
Break size	5%	
Break type	Communicative	
Break location	Cold leg	
Pressurizer location	Intact loop	
Pressurizer line resistance	5.9 x 10^8 m^{-4} d	
ECC Injection		
Upper head accumulator		
Actuation pressure	8.6 ± 0.1 MPa	8.69 MPa
Liquid volume	0.0299 ± 0.0005 m^3	0.0299 m^3 d
Nitrogen volume	0.0299 ± 0.0005 m^3	0.0299 m^3 d
Volume of liquid injected	0.0166 ± 0.0005 m^3	0.0166 m^3 d
Temperature	300 ± 10 K	290 K
Line resistance	2.69 x $10^9 m^{-4}$	
Intact loop accumulator		
Actuation pressure	2.9 ± 0.1 MPa	2.85 MPa
Liquid volume	0.048 ± 0.0005 m^3	0.0456 m^3
Nitrogen volume	0.025 ± 0.0005 m^3	0.0274 m^3
Temperature	300 ± 10 K	290 K
Line resistance	8.59 x 10^8 m^{-4} d	

TABLE 1. (continued)

Parameter	Specified Value	Actual Value
Intact loop HPIS		
Actuation pressure	12.5 ± 0.1 MPa	12.5 MPa
Delay	25 ± 0.5 s	25 s
Injection rate	See Figure 10	
Temperature	300 ± 10 K	290 K
Intact loop LPIS		
Actuation pressure	0.98 MPa ± 0.05 MPa	0.98 MPa
Injection rate	See Figure 10	
Temperature	300 ± 10 K	290 K
Broken loop accumulator		
Actuation pressure	2.9 ± 0.1 MPa	2.87 MPa
Liquid volume	0.016 ± 0.0005 m^3	0.0136 m^3
Nitrogen volume	0.0083 ± 0.0005 m^3	0.01075 m^3
Temperature	300 ± 10 K	290 K
Line resistance	7.73 x 10^9 m^{-4}	
Broken loop HPIS		
Actuation pressure	12.6 ± 0.1 MPa	
Delay	25 ± 0.55	Not used
Injection rate	See Figure 10	
Temperature	300 ± 10 K	
Broken loop LPIS		
Actuation pressure	0.98 ± 0.05 MPa	0.98 MPa
Injection rate	See Figure 10	
Temperature	300 ± 10 K	290 K

a. Approximate value; flow is adjusted to achieve required core ΔT.

b. Secondary side conditions are adjusted to obtain required primary side temperature and ΔT.

c. Figure 10 shows the sum of the scaled flow rates for charging and safety injection pumps.

d. These values are determined by pretest calibrations or through use of process instrumentation.

e. The reported level is the collapsed height of hot water above the top of the tube sheets after the feedwater flow had stopped (24 s after the pressurizer pressure trip). The intact loop feedwater flow averaged 1.6 kg/s and the broken loop feedwater flow averaged 0.64 kg/s.

3. TEST RESULTS

The following sections present a preliminary analysis of the results obtained from Test S-UT-7 data. First, a discussion of general system behavior is presented, followed by more detailed analyses of factors which influenced the response. The primary objective of the experiment was to provide data for the evaluation of the effect of upper head accumulator injection on system response. The evaluation was facilitated by comparison to Test S-UT-6[2] which was performed from similar initial conditions but without UHI, to establish a baseline response for a 5% break.

3.1 General System Behavior

Table 2 presents a sequence of events for Test S-UT-7, derived from test data, which highlights the important operations and thermal-hydraulic events that occurred. System response was characterized by a continuous depressurization and voiding from the upper elevations downward. Formation of loop seals in the pump suctions resulted in a depression of the core liquid level. However, sufficient vessel liquid inventory remained to prevent dryout of the heater rods during this period. The liquid level in the core recovered when the intact loop seal blew out,[a] followed by a small second depression as the broken loop pump suction reformed a seal. Both loops blew out by about 230 s. Boiloff of fluid in the core and downcomer began after the pump suctions had blown out and the cold leg had voided (at about 400 s). A minimum collapsed core level of about 160 cm above the core inlet was reached at 800 s (immediately prior to loop accumulator injection). This resulted in the dryout of approximately the top 60 cm of the core and a brief temperature excursion. The remainder of the transient was characterized by continued system depressurization and a slow filling of the vessel. The injection of ECC into the upper head between approximately 21 s and 296 s resulted in a period of more rapid

---

a. Pump suction liquid seal behavior is generally characterized by a depression of the level in the downflow leg to the bottom of the suction, a rapid "blow out" of about half of the liquid in the upflow leg, followed by a long "clearing" of the remaining liquid.

TABLE 2. SEQUENCE OF EVENTS FOR TEST S-UT-7

Event	Time (s)
Blowdown initiated	0
Pressure trip	8.6
Intact and broken loop main steam valves begin to close	10.8
Upper plenum fluid saturates	11
Core power decay initiated	12.4
Intact and broken loop pump coastdown initiated	14.2
Upper head accumulator injection begins	21
Intact and broken loop main feedwater valves begin to close	34
HPIS initiated	34
Entire system saturated	35
Pressurizer and surge line empty	37
Power to broken loop pump terminated	72.5
Broken loop pump stops	77
Power to intact loop pump terminated	133
Intact loop pump stops	136
Intact loop pump suction blows out and break uncovers	220
Upper head accumulator injection ends	296
Intact loop pump suction cleared of liquid	650
Broken loop accumulator injection begins	738
Intact loop accumulator injection begins	822

TABLE 2. (continued)

Event	Time (s)
Broken loop pump suction cleared of liquid	1600
Broken loop accumulator liquid injection ends	1810
Intact loop accumulator liquid injection ends	3730
Test terminated	4800

system depressurization than was observed in Test S-UT-6. The overall effect of upper head injection on system behavior early in the transient was minimal relative to the response observed in Test S-UT-6. However, the UHI liquid did maintain a minimum core collapsed liquid level 45 cm higher than the 115 cm minimum obtained in Test S-UT-6, significantly improving the margin against severe core heatup.

3.2 Pressure Response

A comparison of the upper plenum pressures for Tests S-UT-6 and S-UT-7 is presented in Figure 11. The timing of events which affected the system depressurization in Test S-UT-7 are indicated on the figure. Upon initiation of the transient, the system underwent rapid depressurization until about 35 s at which time fluid in the entire system became saturated at approximately the initial cold leg temperature. Figure 12 compares the core outlet temperature, and cold leg temperatures to the system saturation temperature and indicates that at about 35 s the cold leg fluid became saturated. Extensive flashing in the primary system is sufficient to reduce the rate of system depressurization since during this portion of the transient the break is still covered with high density fluid.

The primary and secondary side pressure responses for Test S-UT-7 are compared in Figure 13. The responses were very similar for Test S-UT-6. The figure indicates that the intact loop and broken loop steam generators remained thermal sinks for the primary system until 200 s and 250 s respectively. The slow secondary pressure decays for the remainder of the transient indicates that the voiding of the primary side of the tubes acted to effectively decouple primary and secondary behaviors.

The system depressurization response varied between the two experiments due to the UHI system injection in Test S-UT-7. Figure 11 shows that the system pressure dropped more rapidly between approximately 100 and 296 s in Test S-UT-7, during the period of upper head injection. The pronounced drop in pressure in Test S-UT-7 that began at about 225 s

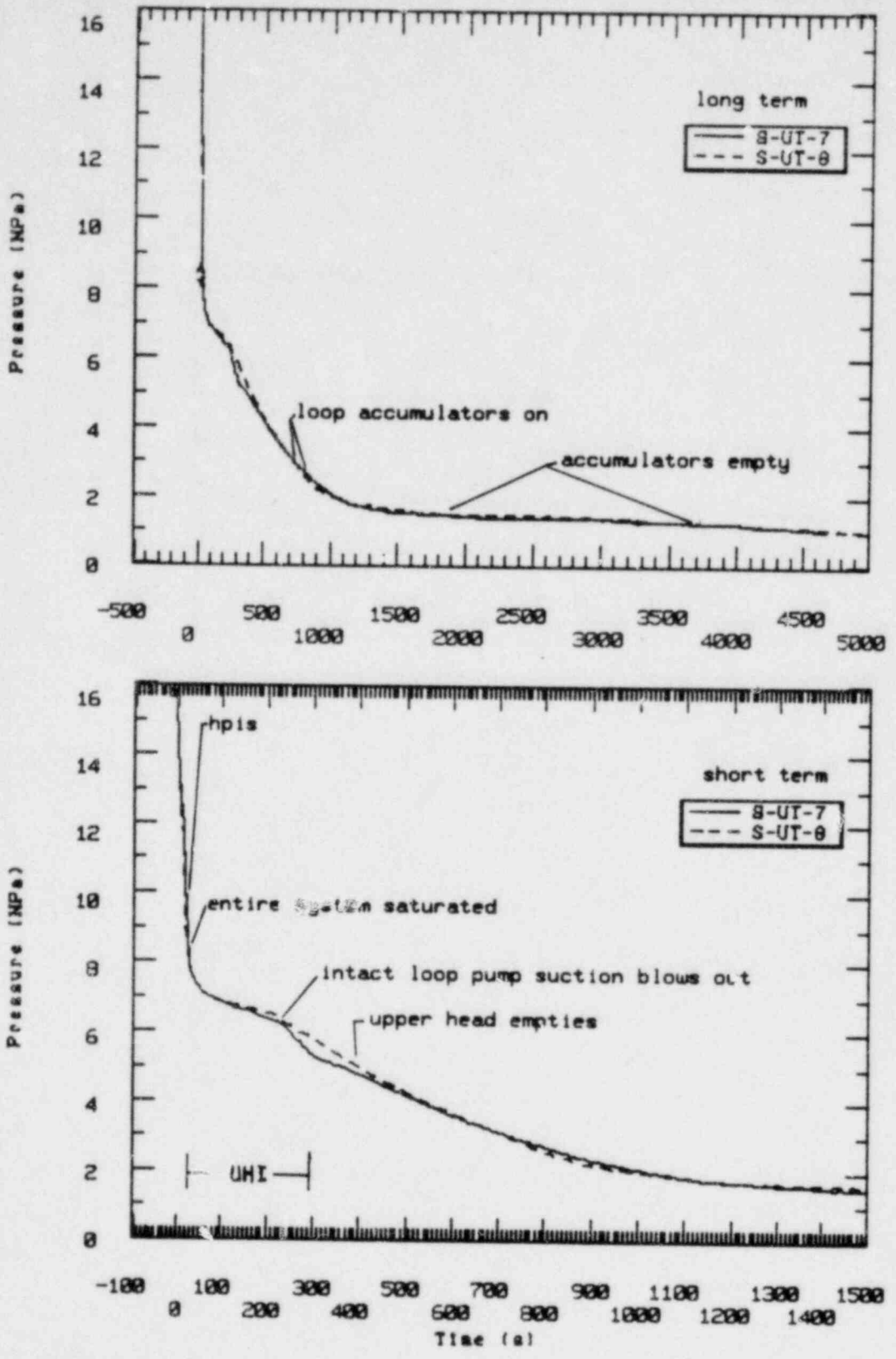

Figure 11. Comparison of the system pressure response for Tests S-UT-6 and S-UT-7.

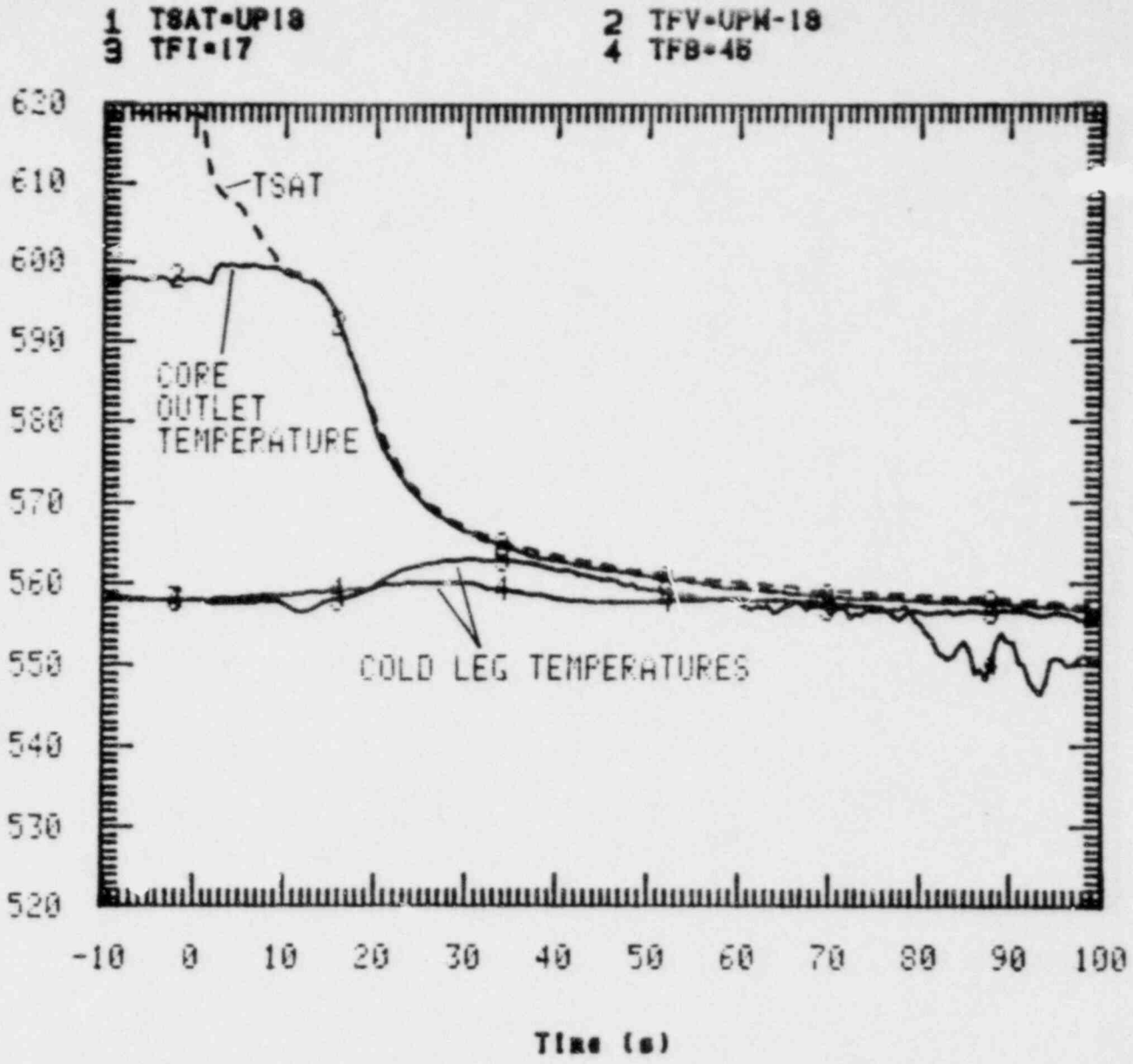

Figure 12. Comparison of selected fluid temperatures to the system saturation temperature.

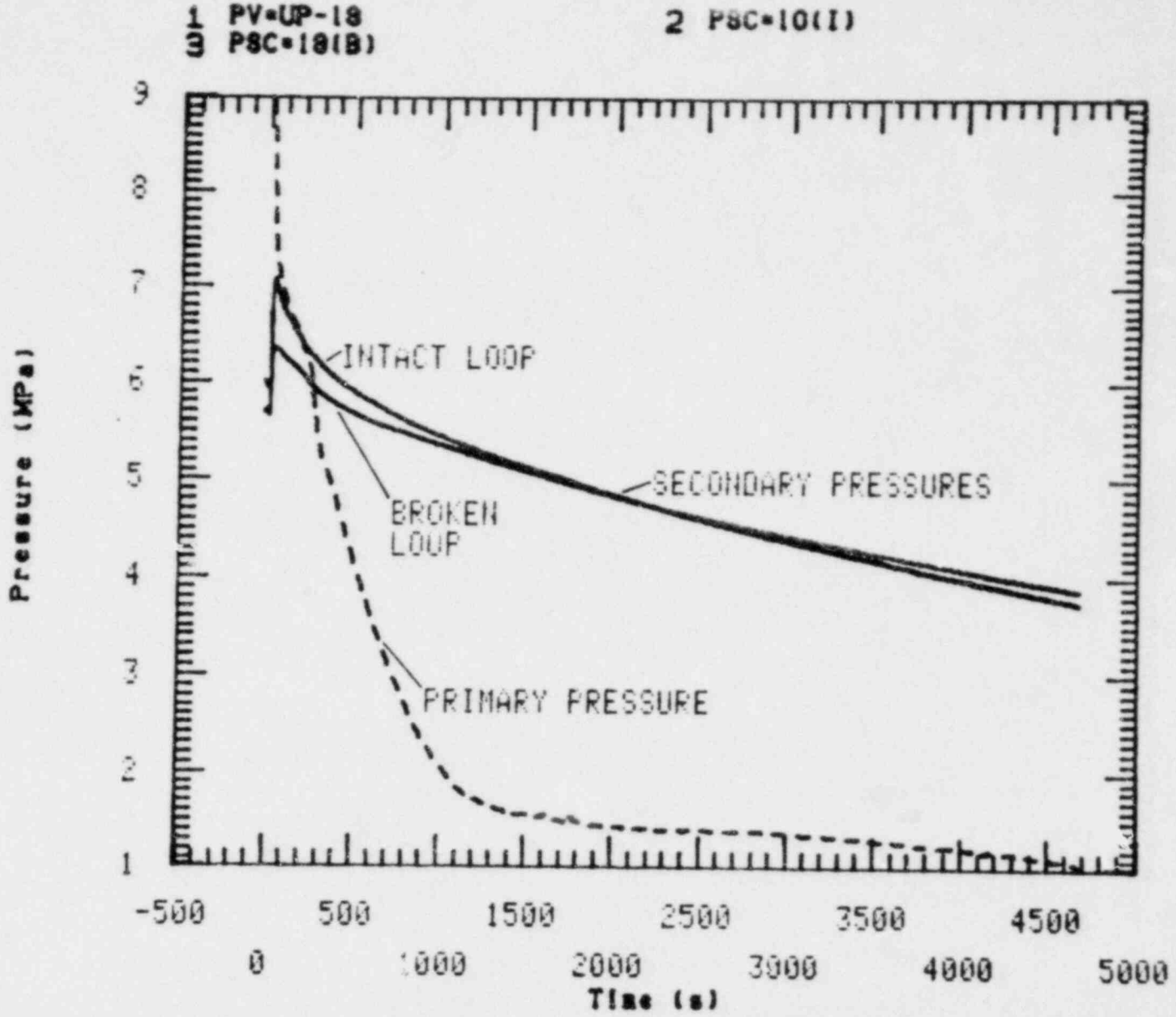

Figure 13. Comparison of primary and secondary side pressure response for Test S-UT-7.

was the result of the voiding of the cold legs and break uncovery which followed pump suction seal blowout. As will be shown in Section 3.3 the cold leg upstream of the break did not void out as extensively in Test S-UT-6. Therefore, while the pressure began to rapidly drop at about the same time in Test S-UT-6 (Figure 11) the depressurization quickly slowed due to the liquid remaining at the break. As liquid from the upper head again filled the cold leg in Test S-UT-7 the depressurization slowed. Since the mass inventory and distribution in Tests S-UT-6 and S-UT-7 were nearly identical after about 400 s the steam generation rates and therefore the depressurization rates were similar.

Loop accumulator injection began at a system pressure of approximately 2.86 MPa and resulted in further slowing of the depressurization rate (see Figure 11). The accumulator injection delivered ECC water to the core and increased the rate of steam generation, resulting in retardation of the system depressurization. The accumulators emptied of liquid by approximately 1810 s and 3730 s in the broken and intact loops respectively, and the rate of depressurization then increased only slightly since the break flow rate and the HPIS rate were nearly identical as shown in Figure 14.

Both experiments were allowed to continue until system pressure reached the LPIS set pressure (0.98 MPa) at 4700 s to verify that for a 5% break experiment core uncovery would not occur prior to introduction of LPIS. At the time LPIS injection began, the collapsed liquid level measurement in the core indicated 90% of the core heated length was covered and the level was stable.

3.3 Break Flow

As shown in Figure 1, a break flow condensing and catch tank system was used to measure the flow out the break during Tests S-UT-6 and S-UT-7. This section discusses preliminary break flow rates as calculated from the catch tank measurements along with a brief explanation of break conditions during the transients.

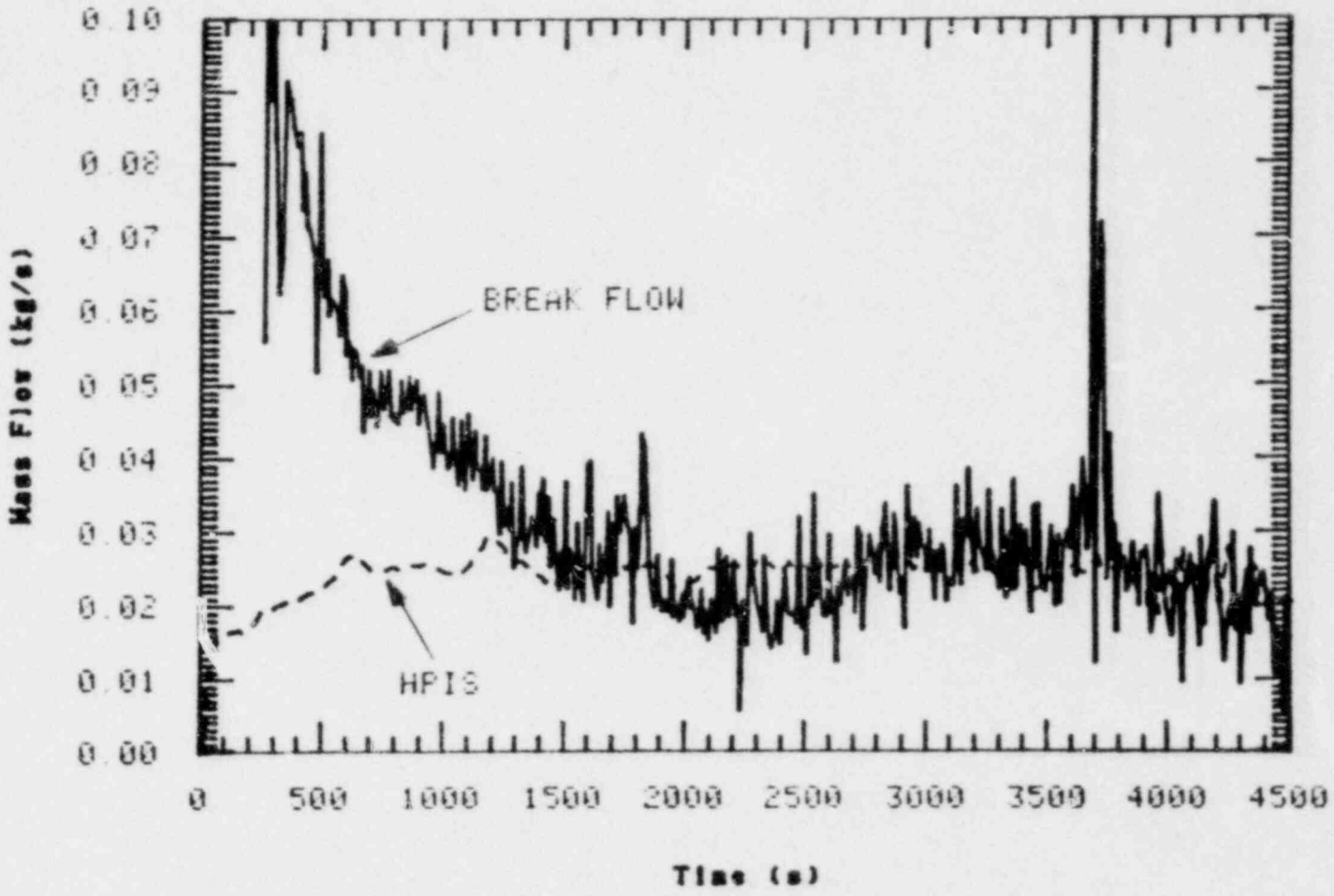

Figure 14. Comparison of the break mass flow and the HPIS flow rate for Test S-UT-7.

Figure 15 compares the mass flow rates out the break for Tests S-UT-6 and S-UT-7. These were calculated by differentiating the liquid level (differential pressure) measurements in the catch tanks. The break flow is characterized as follows. A large initial flow spike occurs at rupture and rapidly decreases as the cold leg fluid approaches saturation at 30 to 40 s. This is followed by a period of relatively high mass flow (saturated high density fluid) until the break begins to uncover at approximately 250 s. This abrupt uncovery is the result of the blowout of liquid in the pump suctions as described in the next section. Thereafter, the break flow consists of primarily high quality steam. Figures 16 and 17 compare the fluid densities in the spool pieces upstream of the break plane in Tests S-UT-6 and S-UT-7 respectively. As can be inferred from the sharp density changes indicated by the middle density shots, the cold leg piping was only partially full of liquid for most of the initial 250 s of the transient, which accounted for the fluctuations in the break flow. While the break initially uncovered at about 230 s in Test S-UT-7 which was earlier than in Test S-UT-6, there was a brief, partial refilling of the cold leg from UHI water as is seen in Figure 17. (Upper head fluid behavior will be discussed in Section 3.6.) The effect of UHI on the break flow rate is illustrated more clearly in Figure 18 which compares the integrated break flow rates for the first 1000 s. It is seen from this figure that the difference in break flows corresponds almost exactly with the amount of UHI liquid injected into the system (16.6 ℓ). The analysis in Section 3.6 will show that it was apparently the case that much of the UHI liquid injected exited the vessel upper head through the bypass line to the downcomer and cold legs. The increased energy removal through the break was the reason for the more rapid depressurization in Test S-UT-7 as discussed in Section 3.2.

The curves in Figure 16 show that some refilling of the broken loop cold leg occurred as a result of loop accumulator injection from approximately 750 to 1300 s. The higher level in Test S-UT-6 probably resulted from the slightly higher injection rates in Test S-UT-6 which resulted from a slightly more rapid depressurization during this time. However, in neither case did the cold leg refill enough to affect the break flow rate.

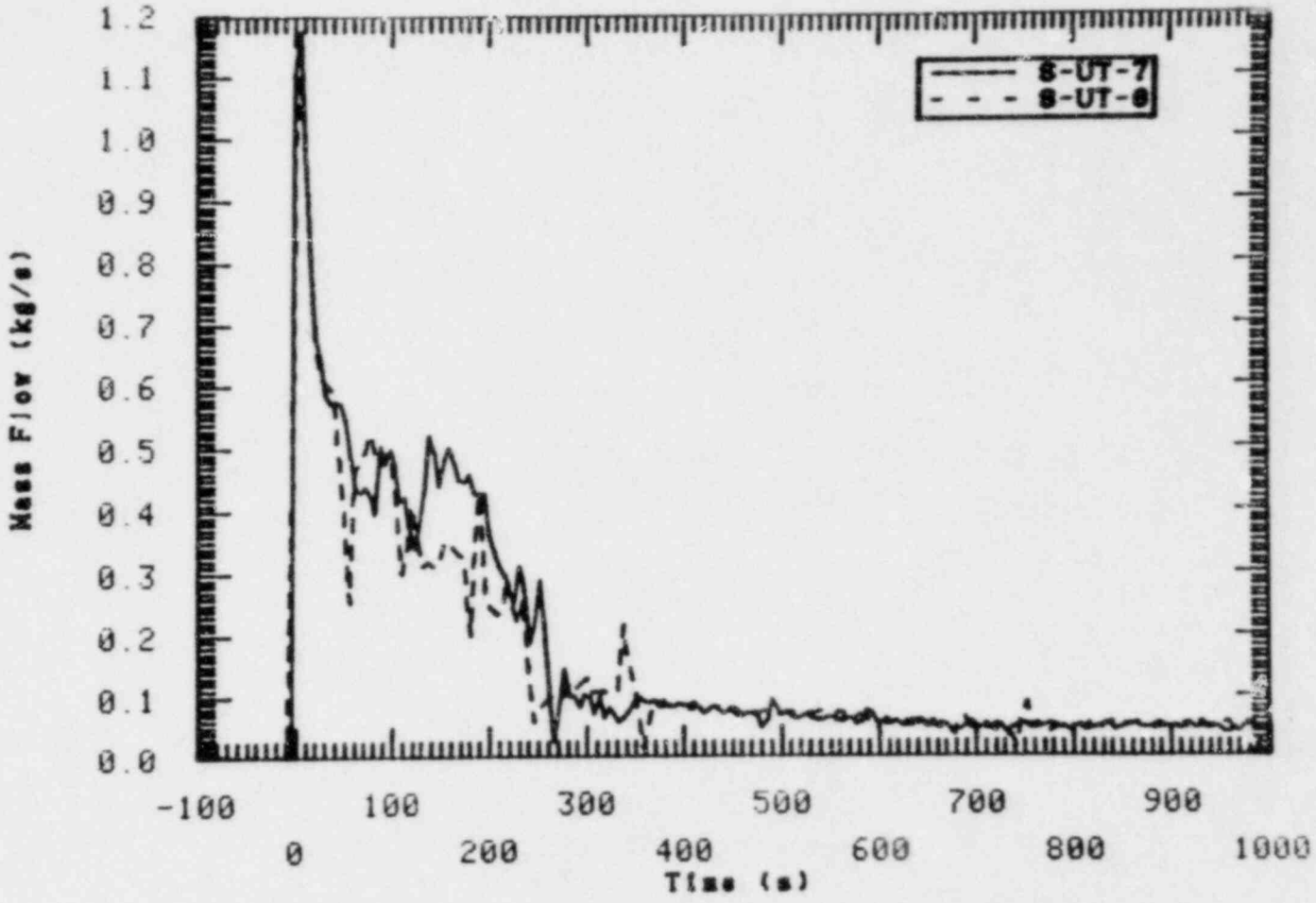

Figure 15. Comparison of break flow rates for Tests S-UT-6 and S-UT-7.

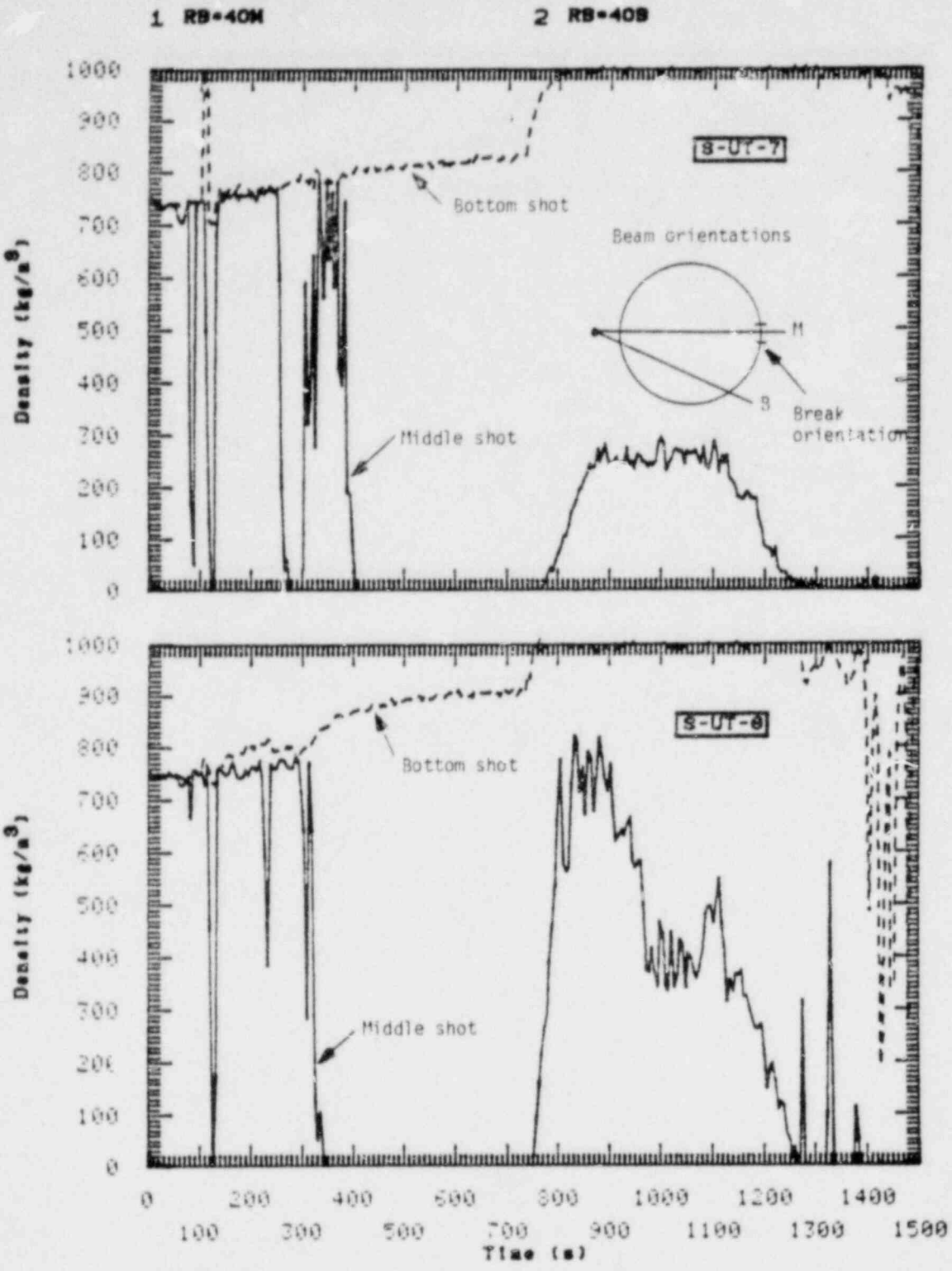

Figure 16. Comparison of fluid densities upstream of the break in spool piece 40 for Tests S-UT-6 and S-UT-7. (Refer to Figure 1 for location relative to break.)

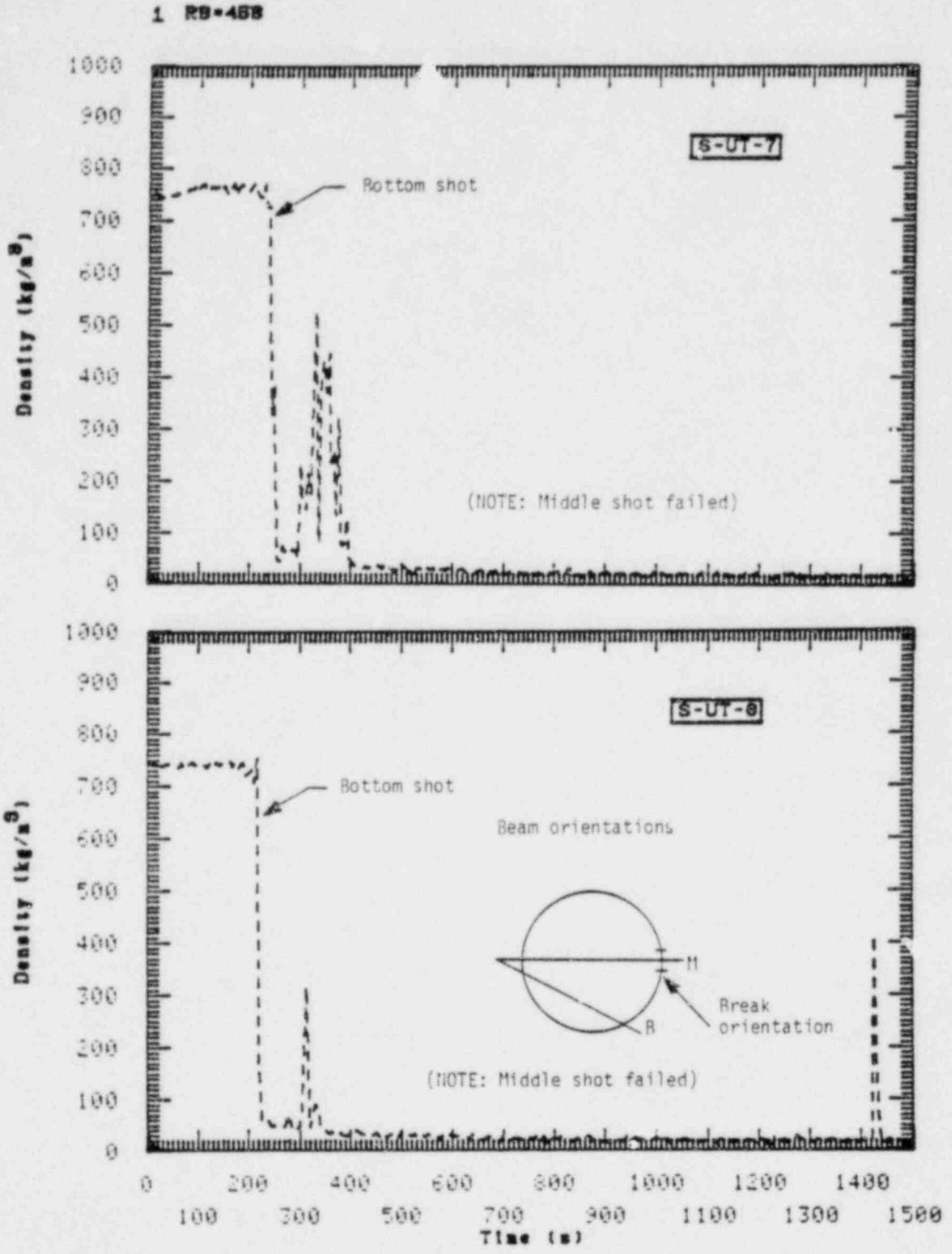

Figure 17. Comparison of fluid densities upstream of the break in spool piece 45 for Tests S-UT-6 and S-UT-7. (Refer to Figure 1 for location relative to break.)

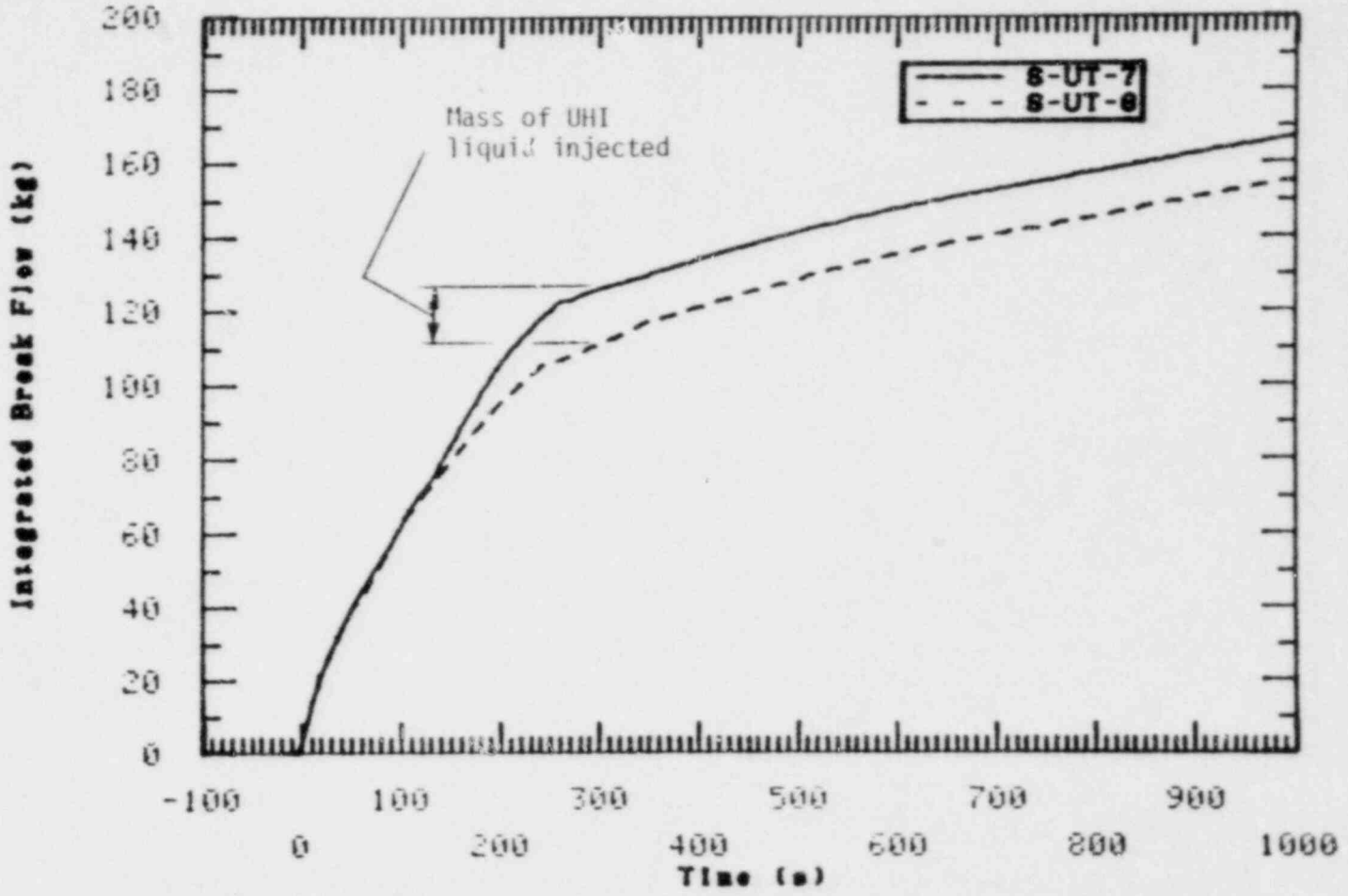

Figure 18. Integrated break mass flows for Tests S-UT-6 and S-UT-7.

The curves in Figure 14 showed that after 1300 s the break flow rate was on the order of the HPIS injection rate. For most of the remainder of the transient the density measurements, as well as video tapes of the break orifice taken through a Storz lens, showed that a small layer of liquid remained in the bottom of the cold leg piping. The break flow was predominantly steam with some apparent entrainment of droplets from the surface of the liquid.

3.4 Loop Hydraulic Response and Void Distribution

The first 250 s of the transient was characterized by the voiding of the loops from the upper elevations downward. Differential pressure measurements showed a smooth, bidirectional collapse of liquid from the top of the steam generator tubes into the loop piping. Measurements in the broken loop steam generator tubes indicated a slower draining than was observed in the intact loop. There was some apparent liquid hold up until about 200 s, versus the approximately 130 s it took the intact loop steam generator tubes to void. Figures 19 and 20 show the liquid level behavior in the intact and broken loop pump suctions, respectively, for Tests S-UT-6 and S-UT-7. Once the liquid levels had collapsed into the suction piping, the remaining liquid formed a manometric "seal" which impeded steam flow around the loops. This in turn caused a back pressure in the core region and some depression of the core level (discussed Section 3.5). By 210 s the level in the intact loop suction was depressed to the bottom of the U-bend and the suction "blew out" most of the liquid in the upflow side. With the establishment of a steam flow relief path around the loop the cold leg piping voided, as was shown in Figures 16 and 17, uncovering the break. The injection of UHI liquid in S-UT-7 had little influence on loop voiding because the injection rate (on the average of 60 m³/s) is small compared to both the break flow rate and the rate of displacement of liquid from the loop piping.

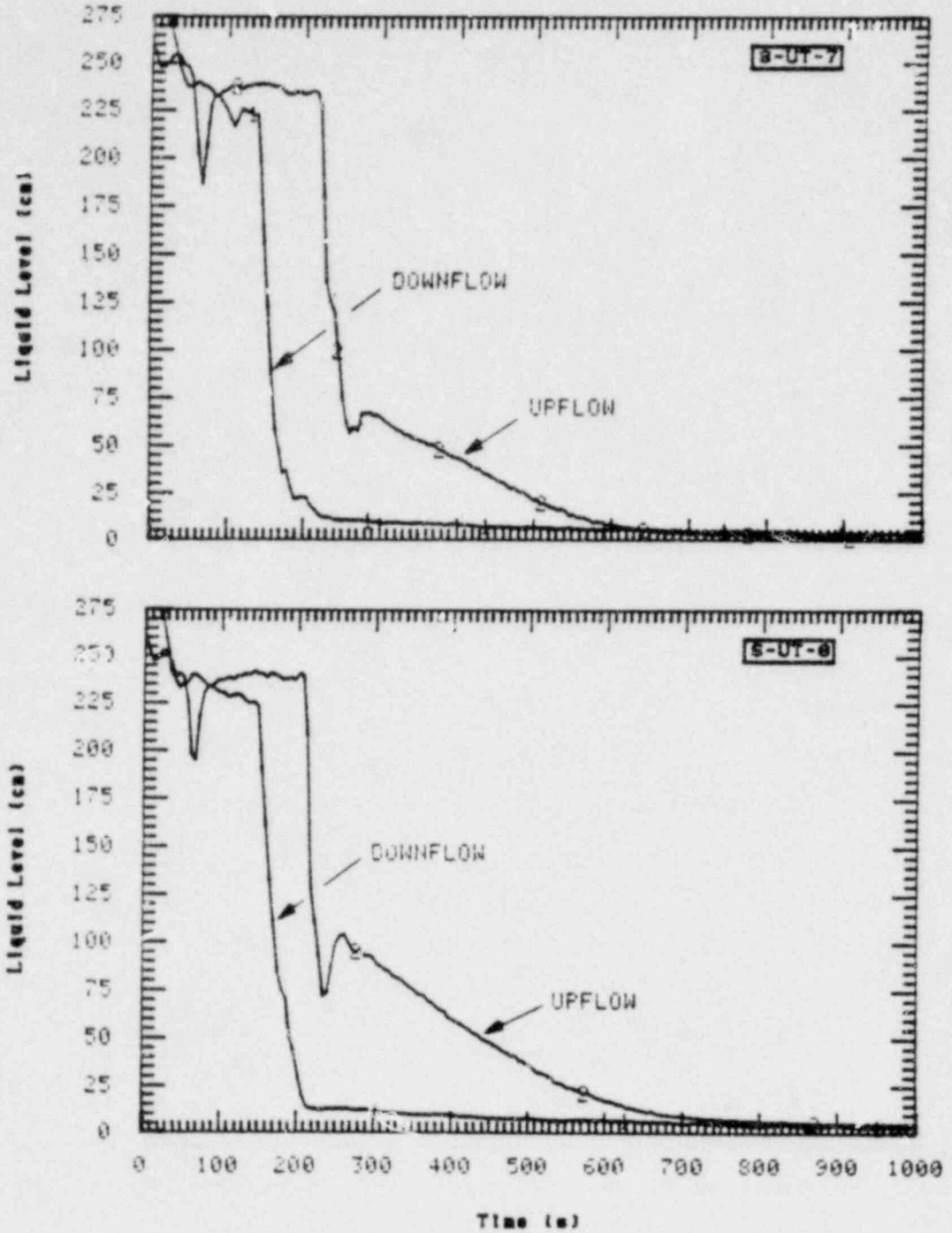

Figure 19. Comparison of collapsed liquid levels in the intact loop pump suction for Tests S-UT-6 and S-UT-7.

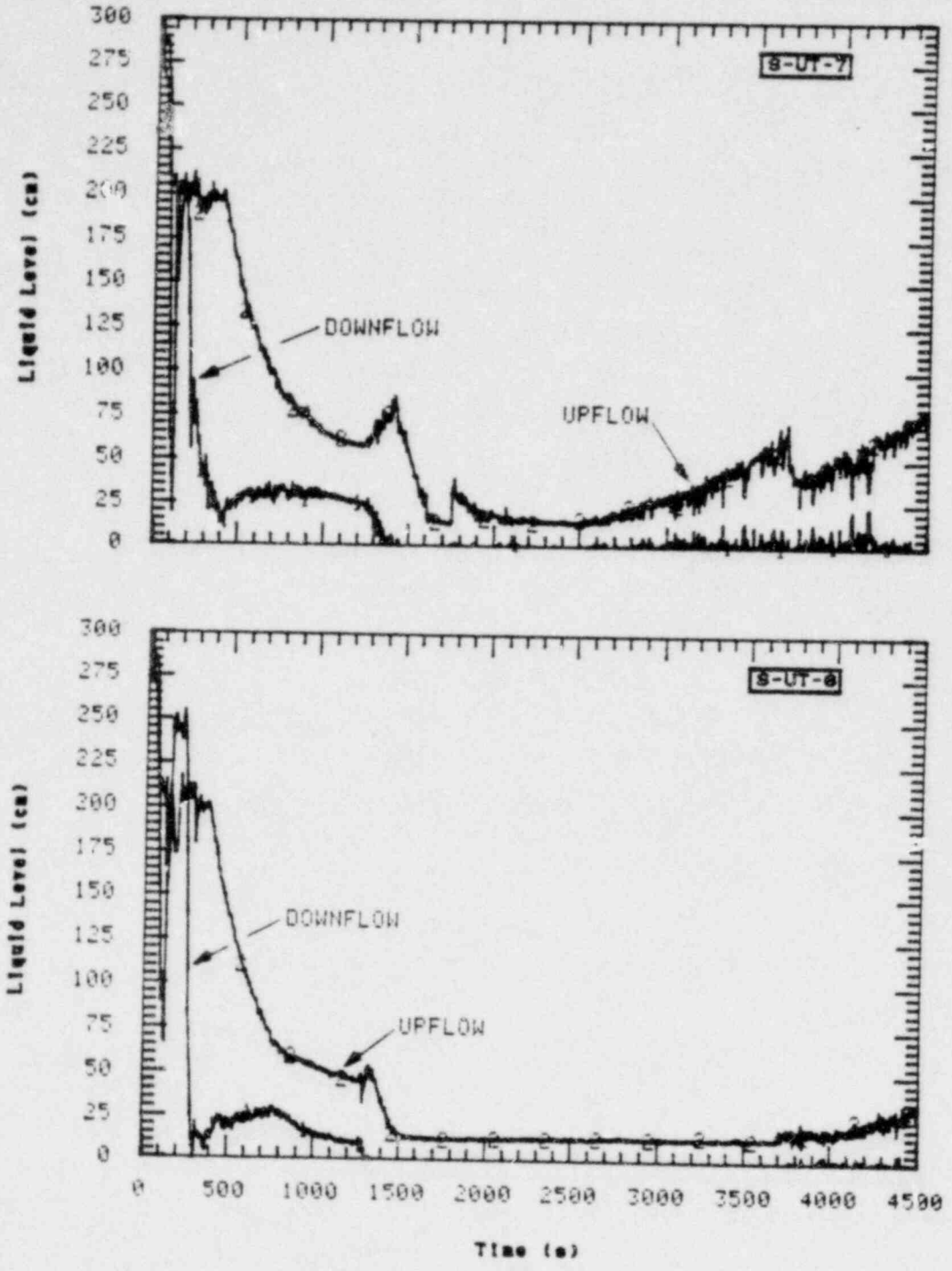

Figure 20. Comparison of collapsed liquid levels in the broken loop pump suction for Tests S-UT-6 and S-UT-7.

The intact and broken loop accumulators began injecting water into the cold legs at 822 s and 738 s respectively. A steady refill of the system accompanied the period of accumulator injection.

A preliminary attempt was made to perform an overall mass balance on the system by balancing the mass flow rates into and out of the system. The component flow rates of the mass balance for S-UT-7 are shown in Figure 21, except for the break flow which was shown in Figure 15. The mass flow rate out of the system (break flow and leakage)[a] was subtracted from the flow into the system (HPIS and upper head, intact, and broken loop accumulators). This net mass flow rate was integrated and added to the 155 kg initial system mass. The results for Tests S-UT-6 and S-UT-7 are compared in Figure 22. Comparison of the two curves with the upper head accumulator flow in Figure 21 shows that the only significant variation in the system masses began at approximately 250 s as a result of the large flow surge from the upper head accumulator. As will be shown in the next section this additional mass had an influence on core behavior, by maintaining a greater vessel liquid inventory. Figure 22 also shows the steady refilling trend of the system which began with accumulator injection. The difference in the two curves after approximately 2500 s is small enough that it may be the result of several approximations used to generate the curves.

3.5 Core Behavior

The vessel liquid inventory in Test S-UT-7 decreased gradually, due to boil off, prior to the initiation of loop accumulator injection and resulted in some heat up of the rods in the upper core region (above approximately 300 cm). Figure 23 compares a typical upper core heater rod temperature response (THV*B4+322) and the core collapsed liquid levels for Tests S-UT-6 and S-UT-7. The data show that in each experiment heatup

---

a. Most of the system leakage occurs through the intact loop pump shaft seals. This leakage was collected for the entire test and an approximate rate estimated as shown in Figure 21.

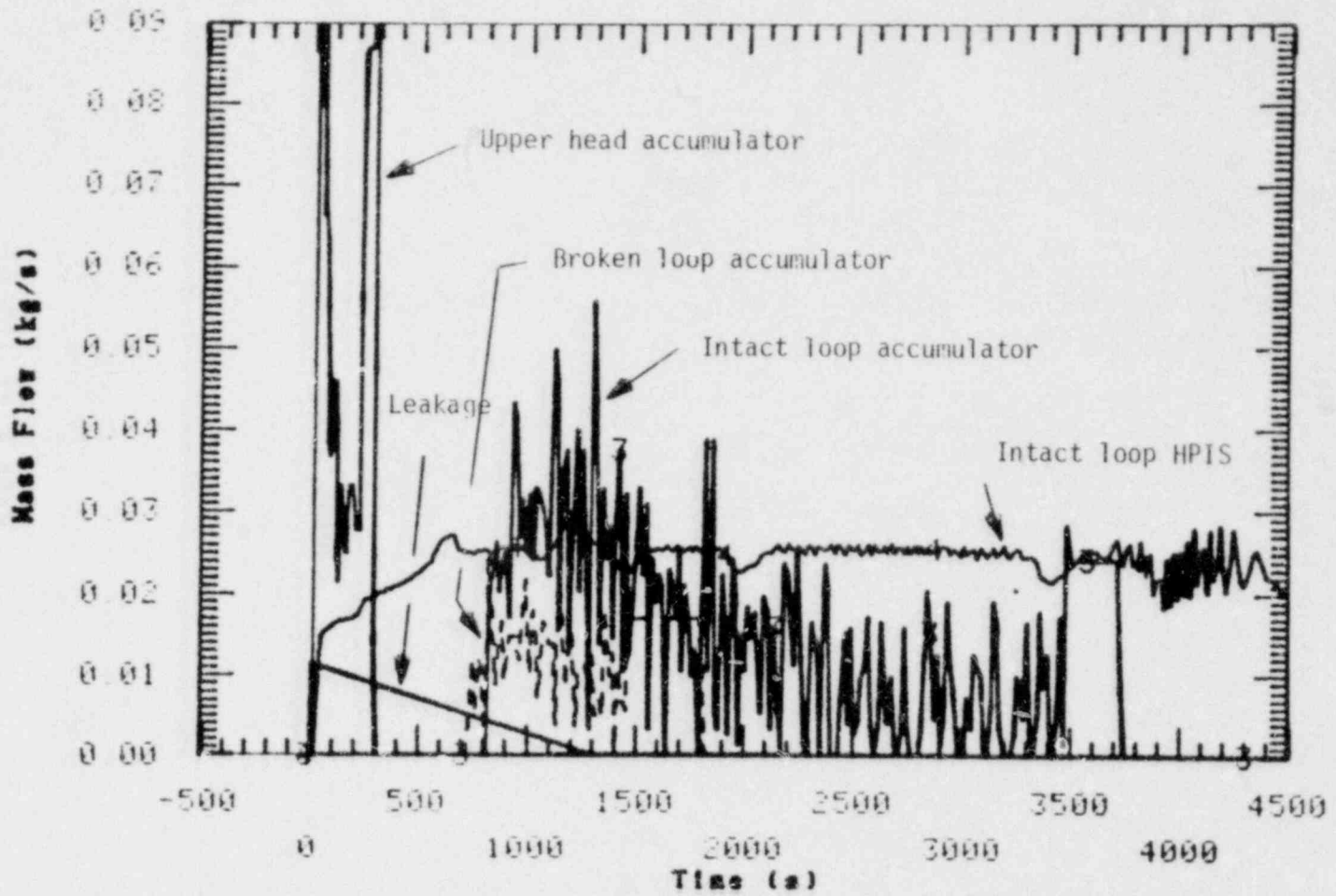

Figure 21. Compenents of system mass balance for Test S-UT-7; system leak rate, HPIS flow rate, upper head, intact, and broken loop accumulator flow rates.

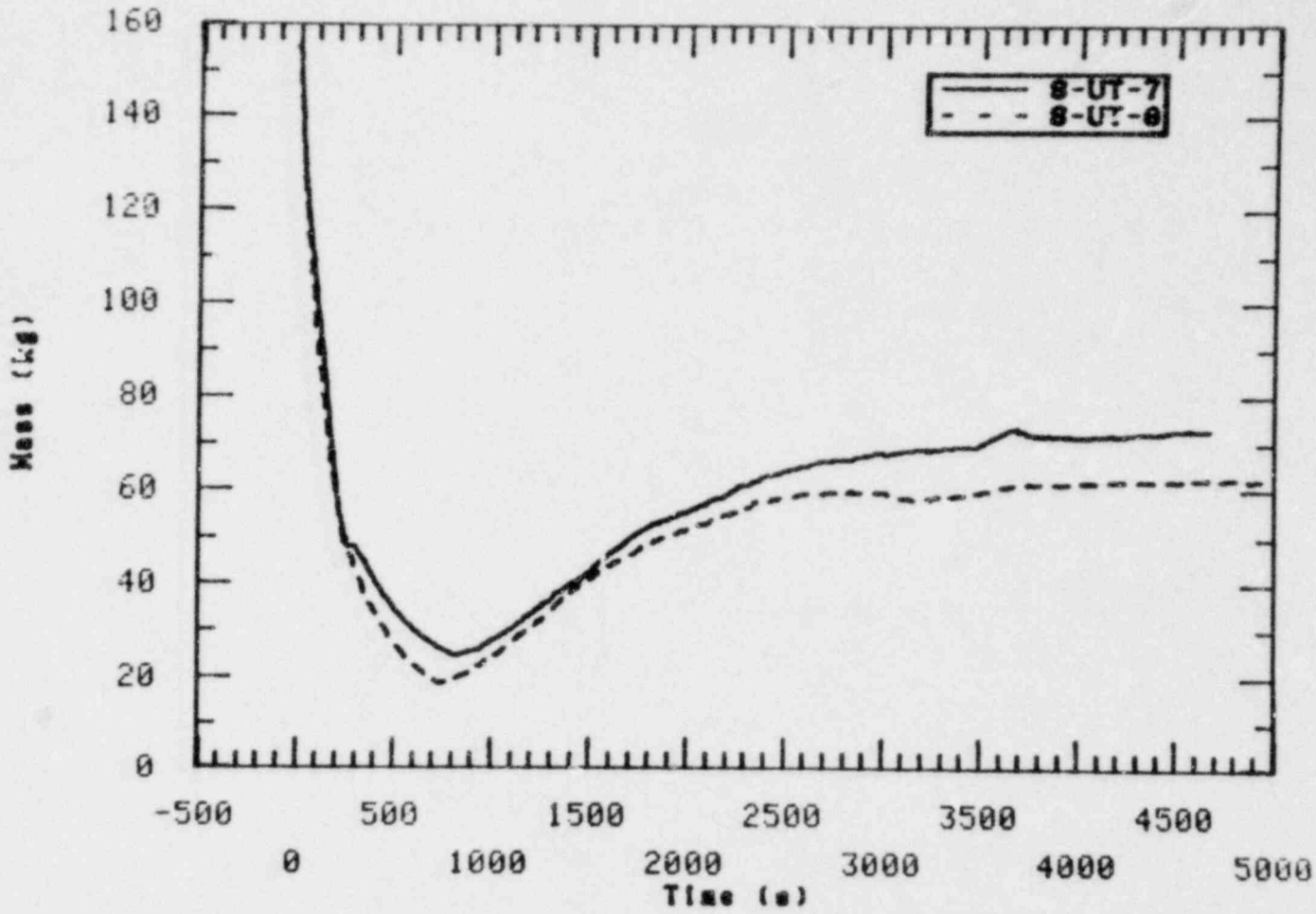

Figure 22. Comparison of system fluid masses for Tests S-UT-6 and S-UT-7.

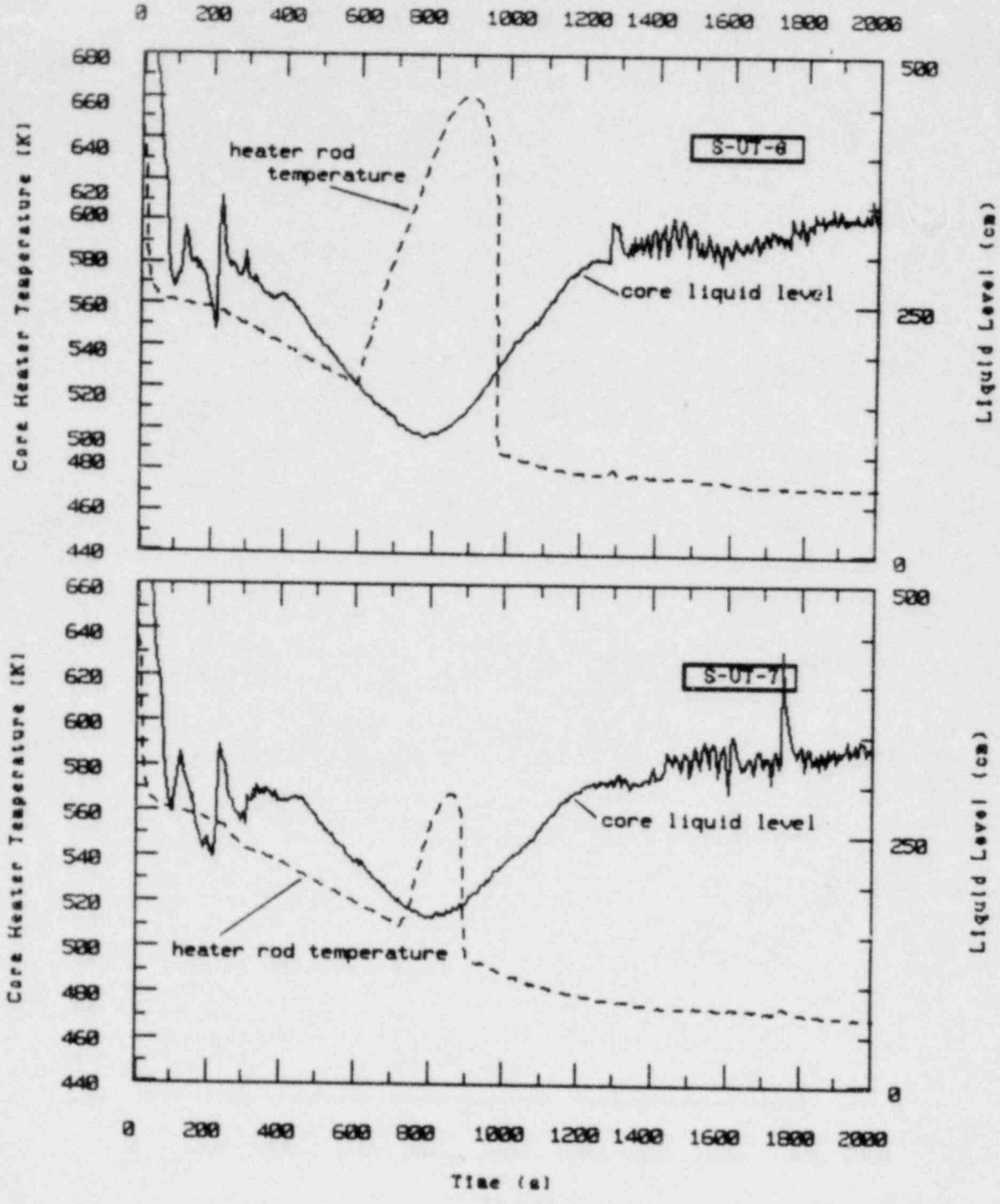

Figure 22 Comparison of the core heater rod response and core liquid level response for Tests S-UT-6 and S-UT-7 (heater rod thermocouple THU * B4+322).

began as the collapsed liquid level reached approximately the middle of the core. Figure 24 compares the collapsed liquid levels in the core and downcomer for Tests S-UT-6 and S-UT-7 and shows that following rupture rapid voiding of the core occurred. Figure 25 further illustrates this core voiding by presenting fluid densities at several elevations in the core (gamma densitometer measurements). The data indicate that within the first 100 s a large axial density gradient was established. Figure 24 shows a higher hydraulic head in the downcomer than in the core for each of the experiments resulting from the formation of loop seals in the pump suctions and from the pressure drop due to flow around the loops. Although in each test the core level was depressed by the formation of loop seals, the depressions were not sufficient to result in any core dryout.

Figure 24 indicates that at about 300 s in Test S-UT-6 a slow boiloff of the core and downcomer liquid inventories began. At about the same time in Test S-UT-7 the core and downcomer inventories increased due to a final drain of upper head liquid, (see the following section) and as a result the level in the core was about 35 cm higher when core boiloff began. The extent of the core boil off that occurred prior to activation of loop accumulator ECC injection directly reflected the replenishing of 35 cm of liquid in Test S-UT-7. The difference in core liquid levels at the point of minimum core inventory was approximately 45 cm. Figure 23 illustrates the benefit of UHI injection in Test S-UT-7 by showing that, although core uncovery and heatup occurred in each experiment, the degree of heatup was considerably less in Test S-UT-7 with typical peak cladding temperatures being approximately 100 K lower.

Once loop accumulator injection began, a steady refilling of the core and downcomer ensued in both tests. In both tests small manometric oscillations occurred between the core and downcomer beginning at about 1250 s which had no effect on core cooling. Following depletion of accumulator liquid the HPIS injection rate in the intact loop was sufficient to replenish boiloff and maintain stable conditions.

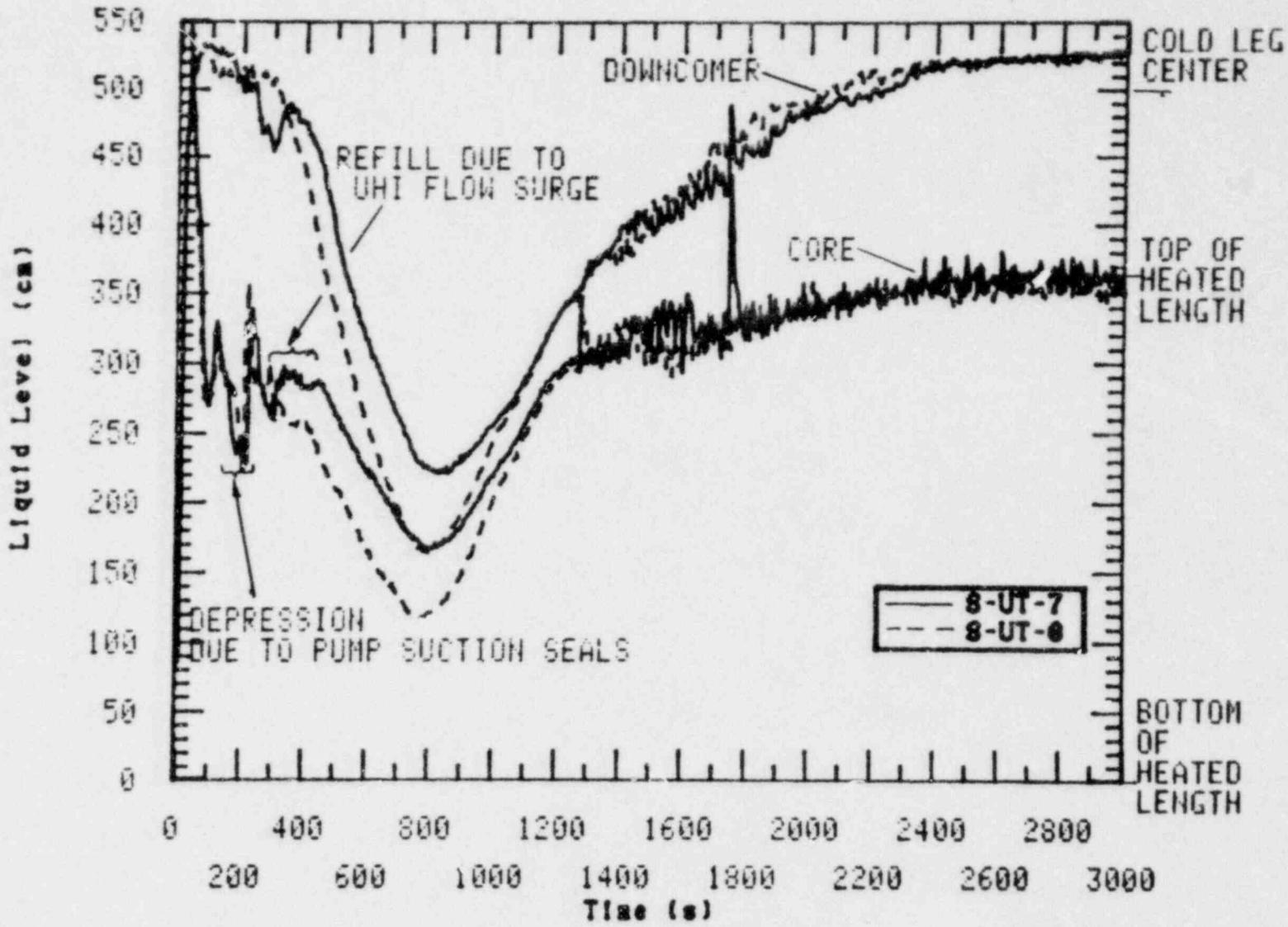

Figure 24. Comparison of the core and downcomer collapsed liquid level response for Tests S-UT-6 and S-UT-7.

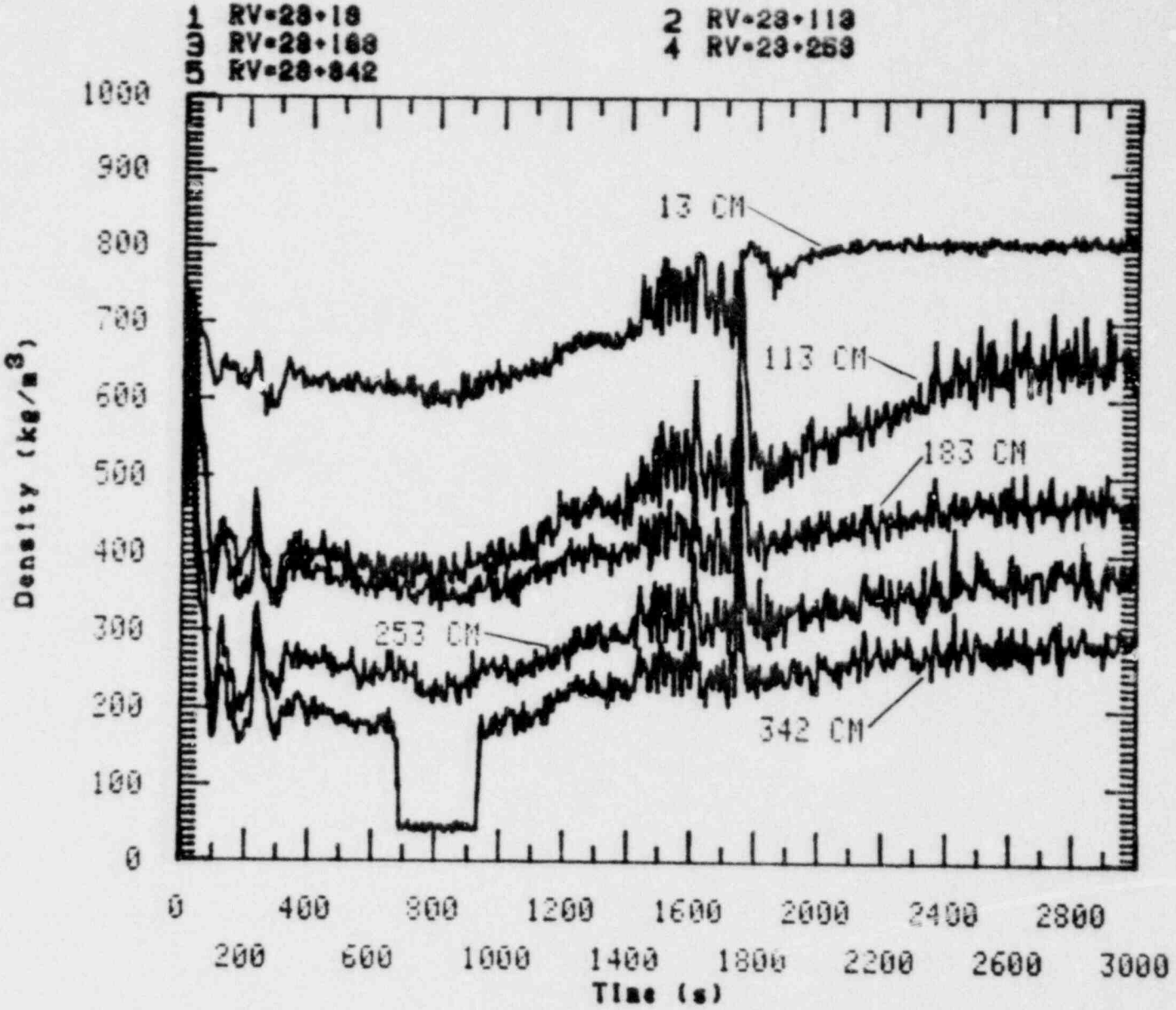

Figure 25. Comparison of in-core density measurements for Test S-UT-7. (Elevations are referenced from the core inlet.)

3.6 Upper Head Fluid Behavior

The distribution of upper head fluid injected from the upper head accumulator is of particular interest in comparing the response in Tests S-UT-6 and S-UT-7. Figure 26 compares the collapsed liquid levels in the upper head for the two experiments. The figure shows that the rate of injection was not sufficient to maintain a full upper head volume and draining occurred. The final draining of the upper head occurred at about 190 s and 400 s in Tests S-UT-6 and S-UT-7 respectively. At about 220 s in Test S-UT-7 the level dropped to the top of the support columns and provided a vent for steam in the core resulting in a sudden drop in pressure. This in turn induced a surge of UHI ECC which nearly refilled the upper head prior to UHI being terminated at 296 s.

Figures 27 through 29 compare the bypass flows, guide tube flows and flows through one support column[a] for Tests S-UT-6 and S-UT-7. The three figures show similar behavior for the first 60 s of the transient as flow through the upper head decays coincident with primary coolant pump coastdown. The bypass flow for Test S-UT-7 (Figure 27) indicates reverse flow (indicating upper head injection and draining) beginning at about 70 s and continuing until about 230 s. At 230 s the upper head liquid level drained below the bypass line elevation and a positive flow of two-phase liquid from the downcomer ensued until about 265 s (due to condensation potential in the upper head) at which time the upper head refilled. Draining of upper head fluid again occurred until about 330 s at which point the bypass line once again cleared. Positive flow continued until the support columns uncovered at about 380 s at which time the upper head, via the bypass line, provided venting of steam generated in the core. The reverse flow through the guide tube (Figure 28) was similar for both experiments until about 125 s. Condensation in the upper head results in reverse flow up the guide tube which increases during the period of 175 s

---

a. The flow measurement in the remaining support column failed in Test S-UT-6.

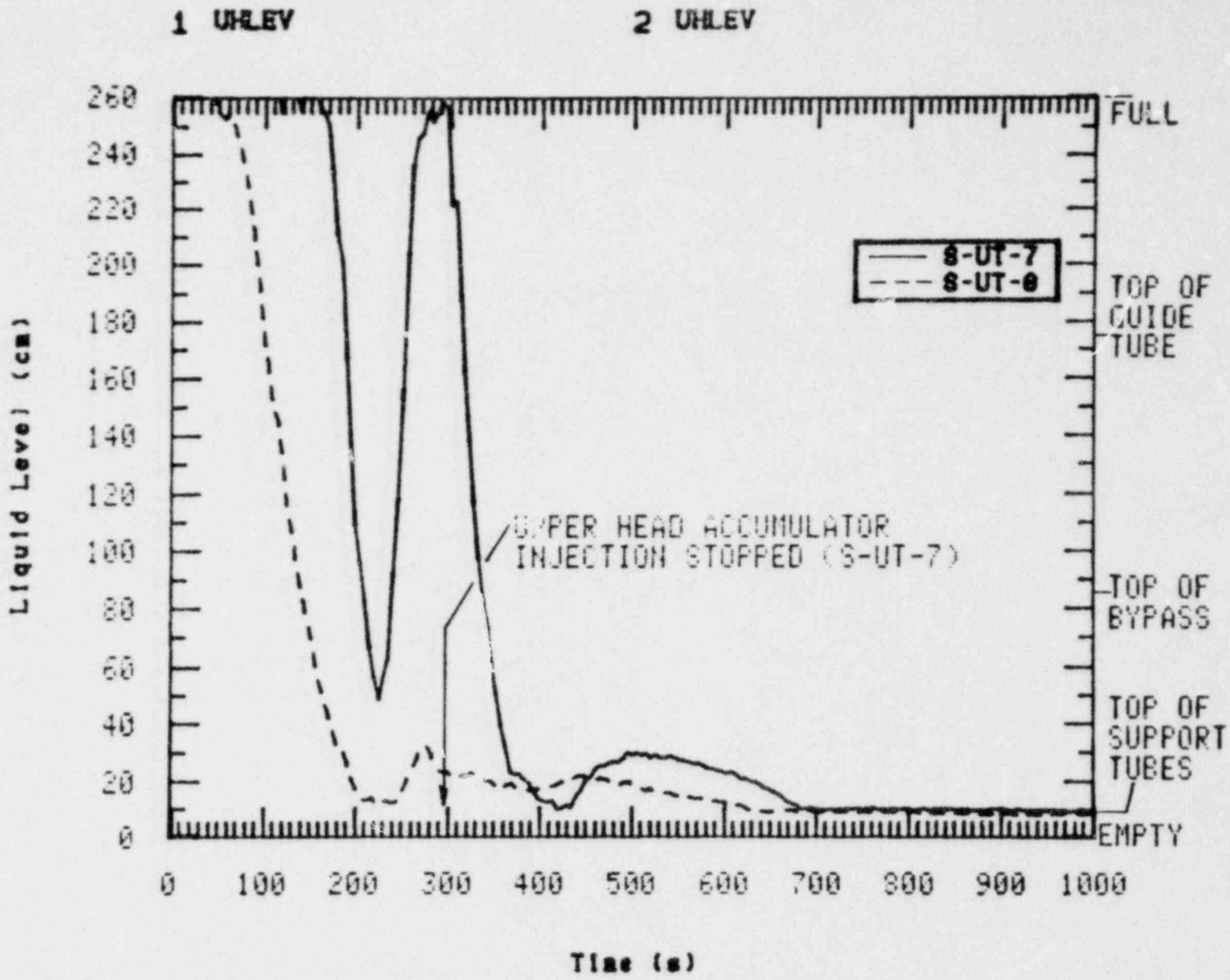

Figure 26. Comparison of the upper head collapsed liquid level for Tests S-UT-6 and S-UT-7.

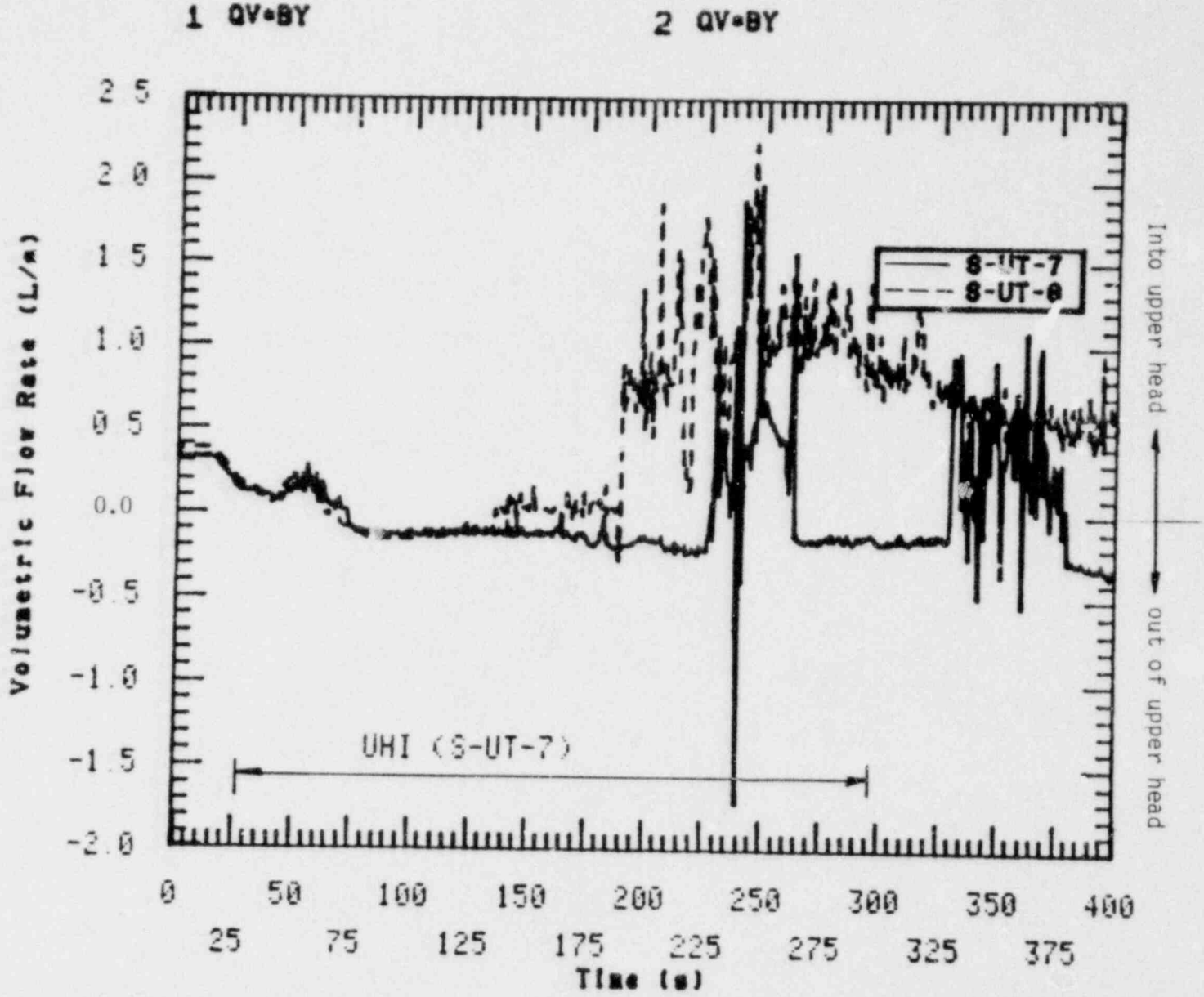

Figure 27. Comparison of the volumetric flow through the bypass line for Tests S-UT-6 and S-UT-7.

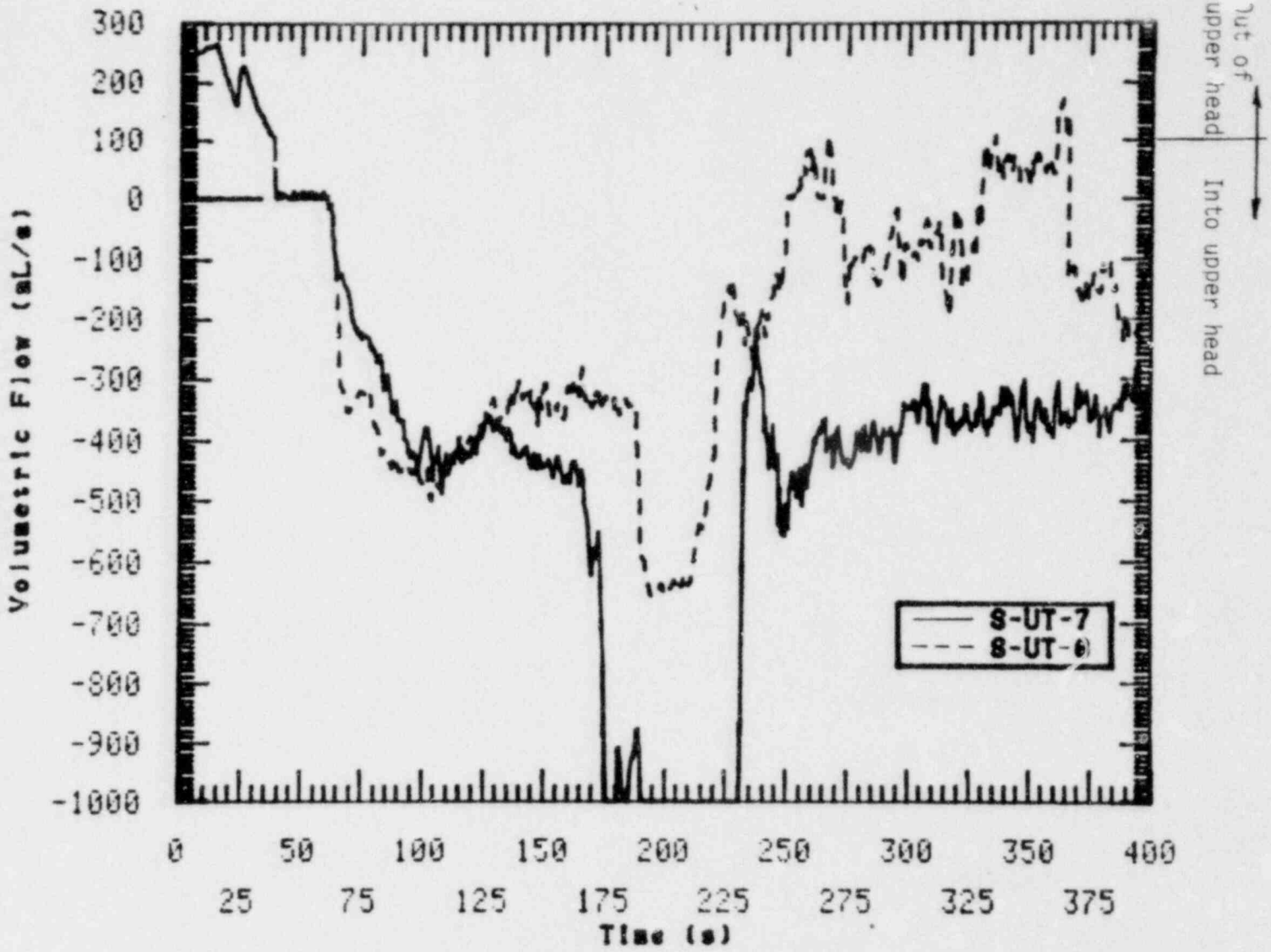

Figure 28. Comparison of the volumetric flow in the guide tube for Tests S-UT-6 and S-UT-7.

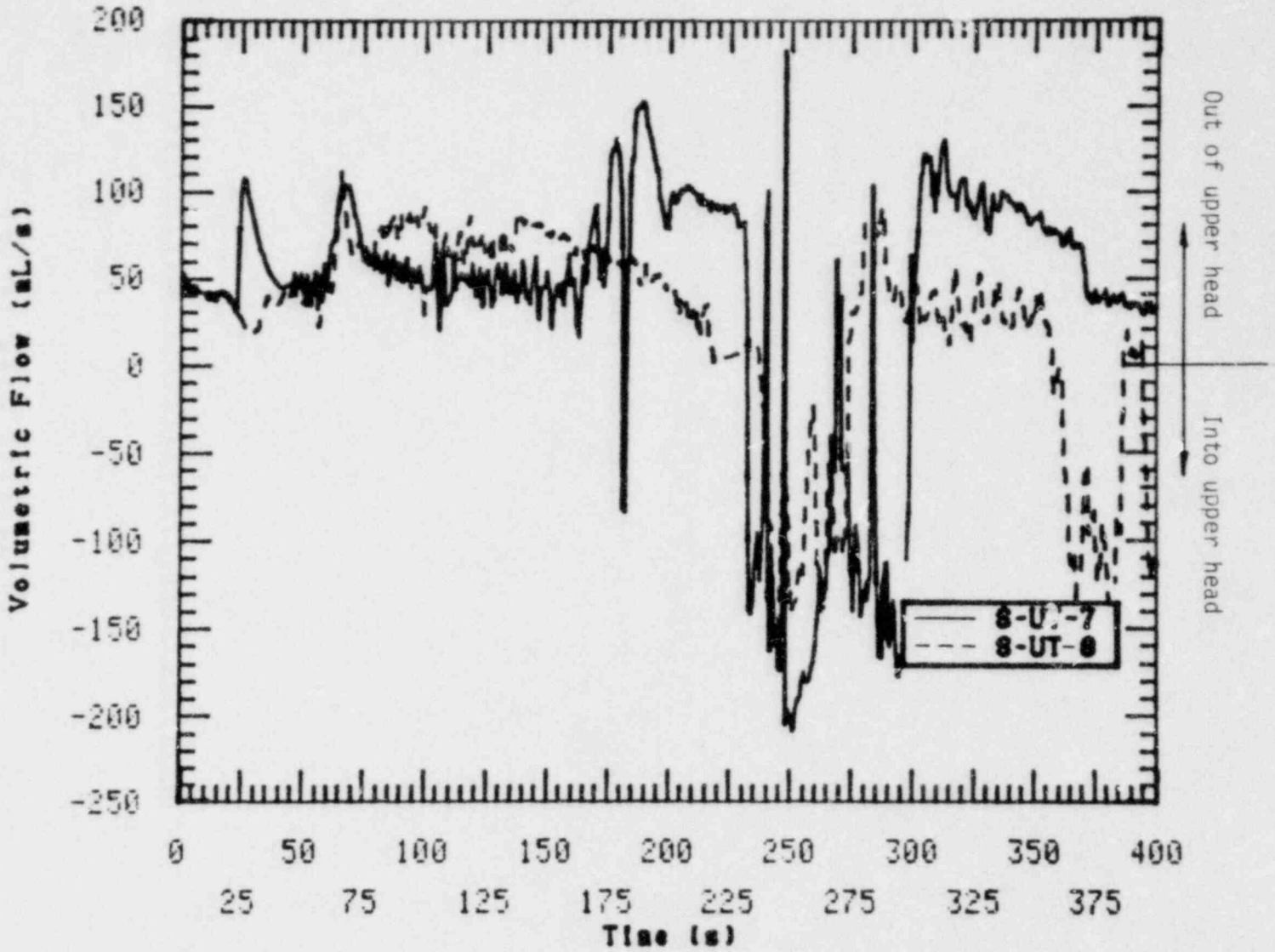

Figure 29. Comparison of the volumetric flow through one of the support tubes for Tests S-UT-6 and S-UT-7.

to 230 s when the collapsed level was below the top of the guide tubes. In Test S-UT-6, the upper head was drained by about 200 s and at that point the reversed flow through the guide tube began to drop to near zero. Support column flow (Figure 29) in Test S-UT-7 remained positive and generally larger than in Test S-UT-6 until the top of the support columns uncovered. At that point, strong reversed steam flow began which persisted until the upper head refill had provided a head of liquid sufficient to re-establish draining. Figure 30 compares the volumetric flow in the two support columns for Test S-UT-7. The figure shows identical behavior in each, except between about 270 s and 300 s during which one tube was draining while the other supported a reversed steam flow. After 296 s, when UHI ended, the subcooling in the upper head decreased which diminished the condensation potential and draining resumed in both support columns.

It is concluded from the upper head fluid behavior, the comparison of core liquid level behavior and thermal response, and the break flow response that the UHI liquid provided energy removal from the system by directly increasing the break flow rate. The UHI also increased the core and downcomer liquid inventory after the pump suction piping liquid blew out, prior to core boiloff. The net effect was reflected in a core heatup in the upper core region that was about 100 K less than in the non-UHI experiment.

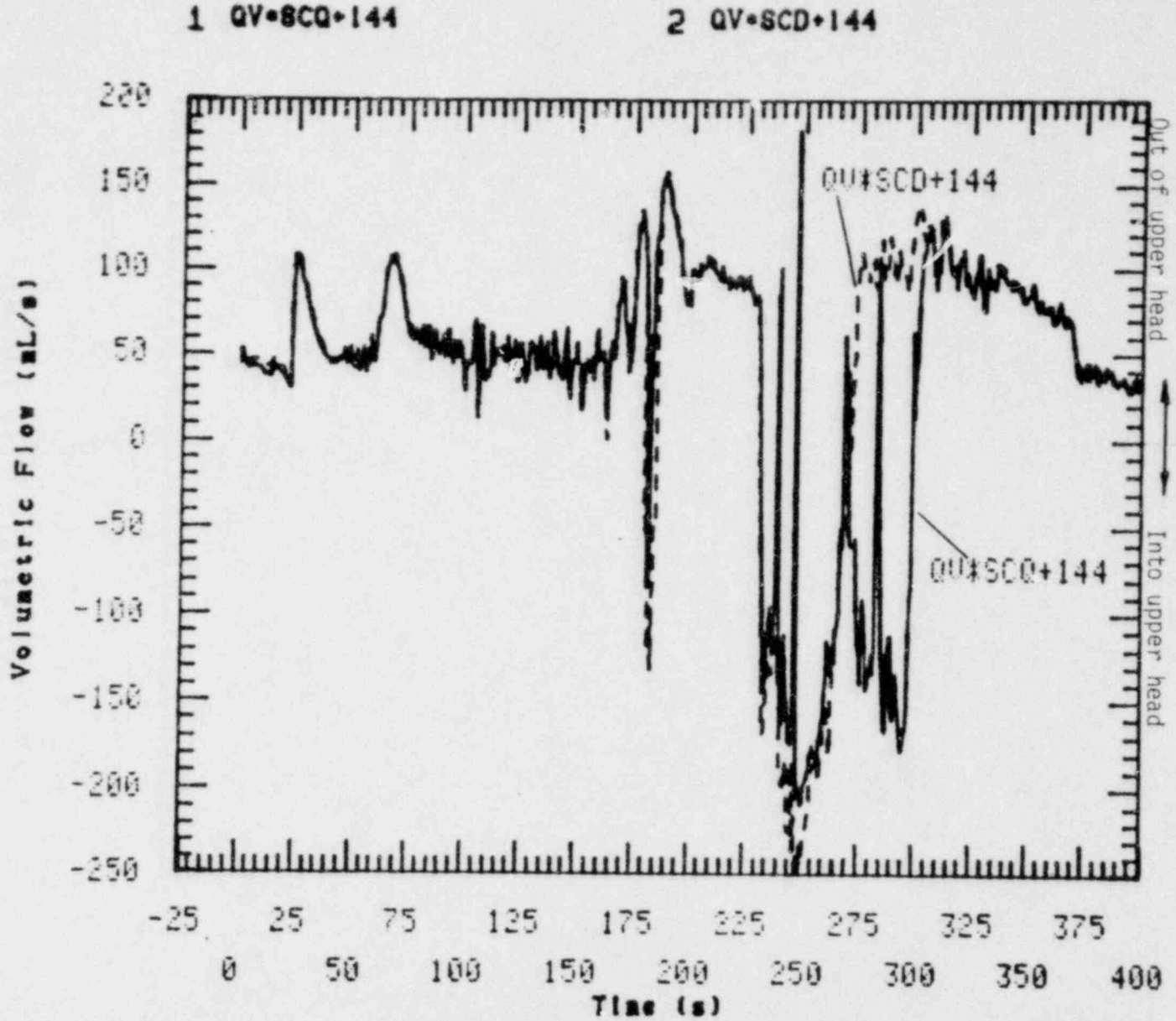

Figure 30. Comparison of the volumetric flow through the two support tubes for Test S-UT-7.

4. COMPARISON OF SELECTED DATA TO PRETEST PREDICTION CALCULATION

A comparison of Test S-UT-7 data to results of the test prediction is presented in this section. The test prediction calculation was performed through the first 782 s of the transient using the RELAP5/MOD1 computer code (Version 6). A detailed description of the results of the calculation is given in Reference 4. The system model used in the calculation is described in Appendix A. Comparisons presented in this section provide a basis for evaluating the capability of the present analytical model to predict the system response resulting from a 5% communicative cold leg break with UHI in the Semiscale Mod-2A facility. Table 3 compares the significant initial conditions specified, measured, and calculated for Test S-UT-7; Table 4 shows the calculated sequence of events for Test S-UT-7.

The most significant difference between the calculation and the experiment was that the calculated velocity of the vapor phase flowing through the break was apparently too high after the transition to a two-phase break flow occurred at 189 s. This is believed to have been caused by the use of 0.9 for the two-phase discharge coefficient at the break junction. The appropriate value of the two-phase discharge coefficient depends on the shape of the break orifice and is not known precisely. The approximate range of values for a rounded entrance orifice (used at the break in Test S-UT-7) is 0.7 to 0.9. The effect of the break two-phase discharge coefficient on calculated system response will be investigated as part of the posttest analysis effort.

As a result of the high vapor velocity at the break, the system pressure was underpredicted after transition to two-phase break flow at 189 s in the calculation (Figure 31). From 0 to 189 s the calculation agreed reasonably well with the experiment; however, Figure 31 shows that after flashing started in the primary system at 30 s, the calculated rate of depressurization was slightly higher than the measured rate. The clearing of liquid from the broken loop pump suction piping (Figure 32) at 230 s in the calculation resulted in the formation of a vapor path from the

TABLE 3. INITIAL CONDITIONS FOR TEST S-UT-7

	Specified	Measured	RELAP5
Nominal system pressure	15.5 ± 0.2 MPa	15.5	15.5
Hot leg fluid temperature	594 ± 2 K	598	594
Cold leg fluid temperature	557 ± 2 K	558	558
Total core power	2.0 ± 0.005 MW	2.0	2.0
Core inlet flow rate	9.77 kg/s[a]	9.0	9.31
Steam generator secondary pressure			
Intact loop	5.9 ± 0.2 MPa[b]	5.70	5.45
Broken loop	5.9 ± 0.2 MPa[b]	5.92	5.44
Steam generator secondary water level			
Intact loop	Footnote b	680	467
Broken loop	Footnote b	650	677
Steam generator secondary feedwater Temperature			
Intact loop	495 ± 2 K	502	495
Broken loop	495 ± 2 K	497	495

a. Approximate value; flow is adjusted to acnieve required core ΔT.

b. Secondary flow conditions are adjusted to obtain required primary side temperature and ΔT.

TABLE 4. SEQUENCE OF EVENTS FOR TEST S-UT-7

Event	Calculated Time (s)	Measured Time (s)
Break opens.	0.0	0.0
Scram signal received (low pressure).	8.6	8.6
Steam generator steam valves begin to close.	8.6	10.0
Hot legs reach saturation.	10.0	11.0
Core power trips, primary coolant pumps trip.	12.0	12.4
Pressurizer empties.	20.0	37.0
Start of UHI accumulator injection.	24.0	21.0
Intact loop cold leg reaches saturation.	31.0	35.0
HPIS initiates.	33.6	34.0
Broken loop primary coolant pump completed coastdown.	82.0	77.0
Intact loop steam generator becomes a heat source.	100.0	200.0
Intact loop primary coolant pump completed coastdown.	142.0	136.0
Broken loop steam generator becomes a heat source.	190.0	250.0
Intact loop pump liquid seal clears.	260.0	220.0
Start of intact loop accumulator injection.	520.0	822.0
Start of broken loop accumulator injection.	520.0	738.0
End of calculation.	782.0	

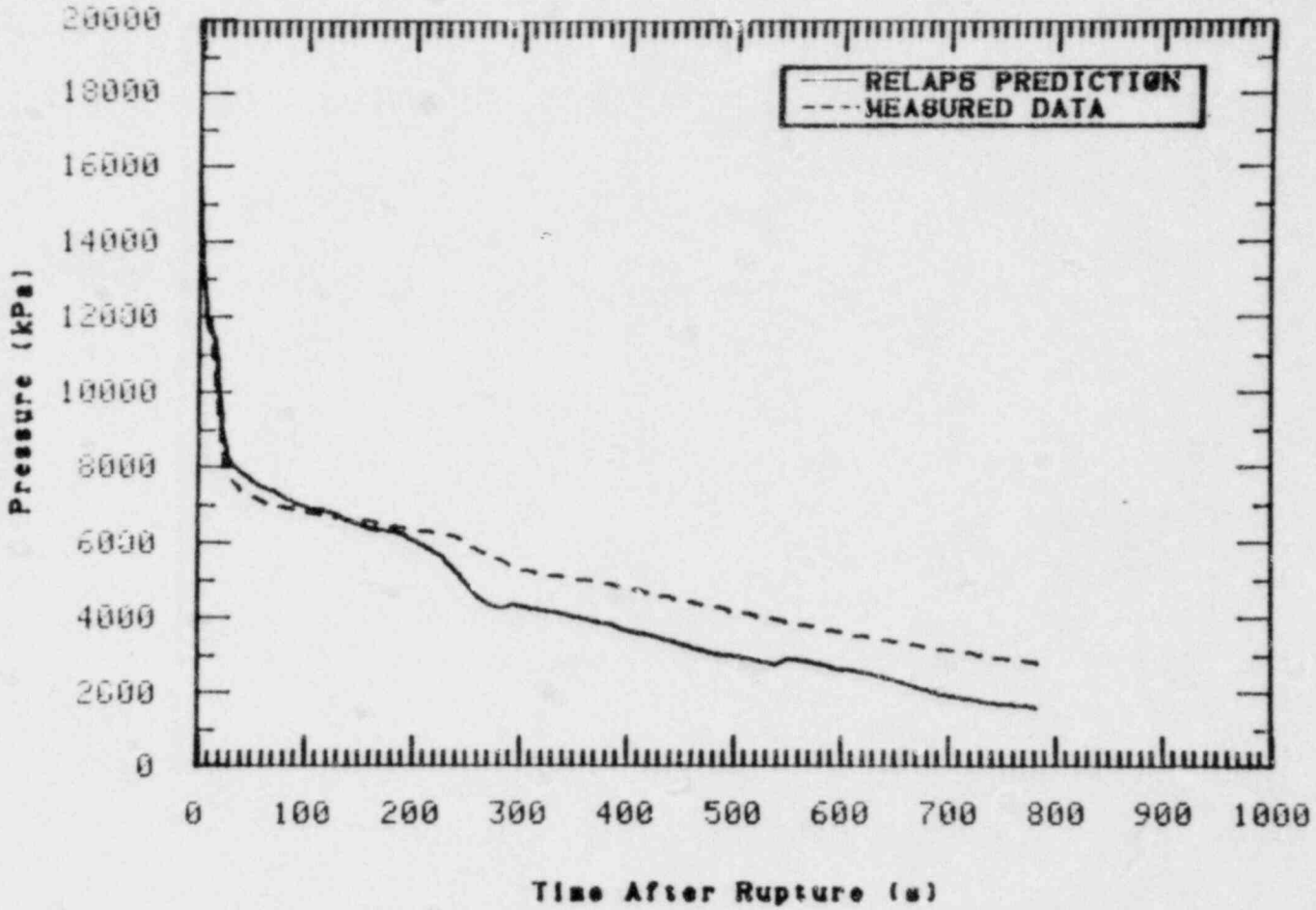

Figure 31. Comparison of calculated and measured system pressure for Test S-UT-7.

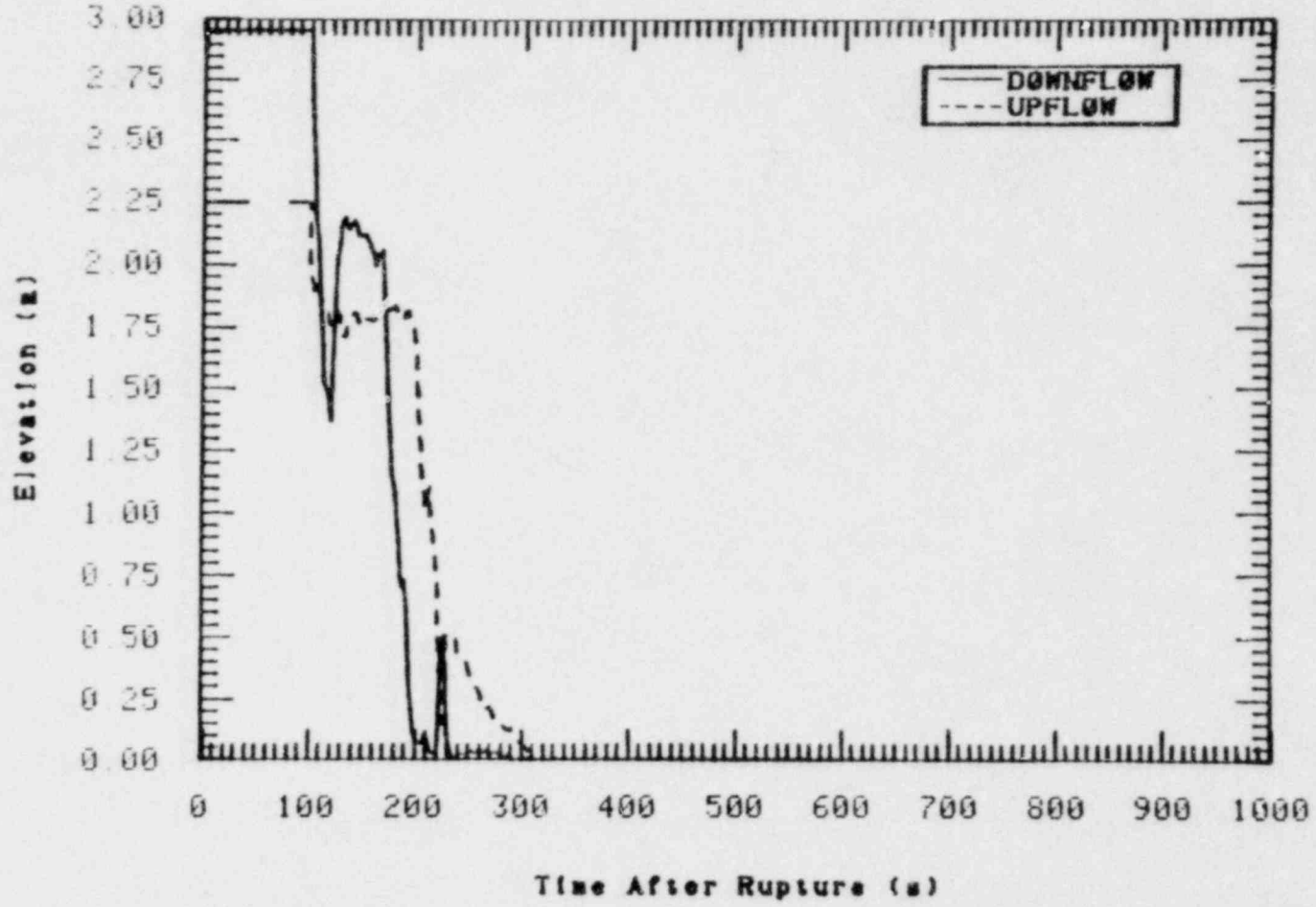

Figure 32. Calculated broken loop pump suction collapsed liquid levels for Test S-UT-7.

vessel to the break. This resulted in an increased volumetric flow through the break which then caused a higher rate of depressurization in the calculation at 230 s. In the experiment, the intact loop pump suction cleared at 250 s (Figure 19). Figure 31 shows a corresponding increase in the rate of depressurization in the experiment at this time. In both the experiment and calculation, the rate of depressurization decreased after draining of the upper head (Figure 33), which occurred at 320 s in the experiment and 280 s in the calculation. The reduction in depressurization rate was caused by increased vapor generation when the upper head fluid drained into the hotter regions of the vessel.

The underprediction of the system pressure (Figure 31) after 150 s resulted in earlier activations of the loop accumulators (Figure 34). The initial calculated effect of the accumulator injection at 520 s was to increase the liquid inventory in the cold legs. The increased density upstream of the break resulted in a reduction of the break volumetric flow. With the reduced break volumetric flow, the calculated vapor generation rate in the core at this time was sufficient to briefly increase the system pressure. The increase in system pressure in the calculation caused the accumulator to shut off from 550 to 580 s as shown in Figure 34.

The system mass inventory (Figure 35) was generally predicted well from 0 to 520 s. At 520 s the loop accumulators were activated and the system mass was over predicted after this time. The overprediction of the vapor velocity at the break after 189 s resulted in the overprediction of vapor generation and liquid depletion in the vessel. Figure 36 shows that two periods of core boiloff occurred in the calculation which were not observed in the experiment. The first period was terminated at 280 s by the draining of the upper head, and the second ended at approximately 600 s as a result of the cold leg accumulator injection. Both of the calculated boiloff periods resulted in brief temperature excursions. These are shown in Figure 37 which compares the highest calculated cladding temperature with the corresponding measurement. (The initial measured temperature is higher in Figure 37 because it is an internal temperature; the calculated

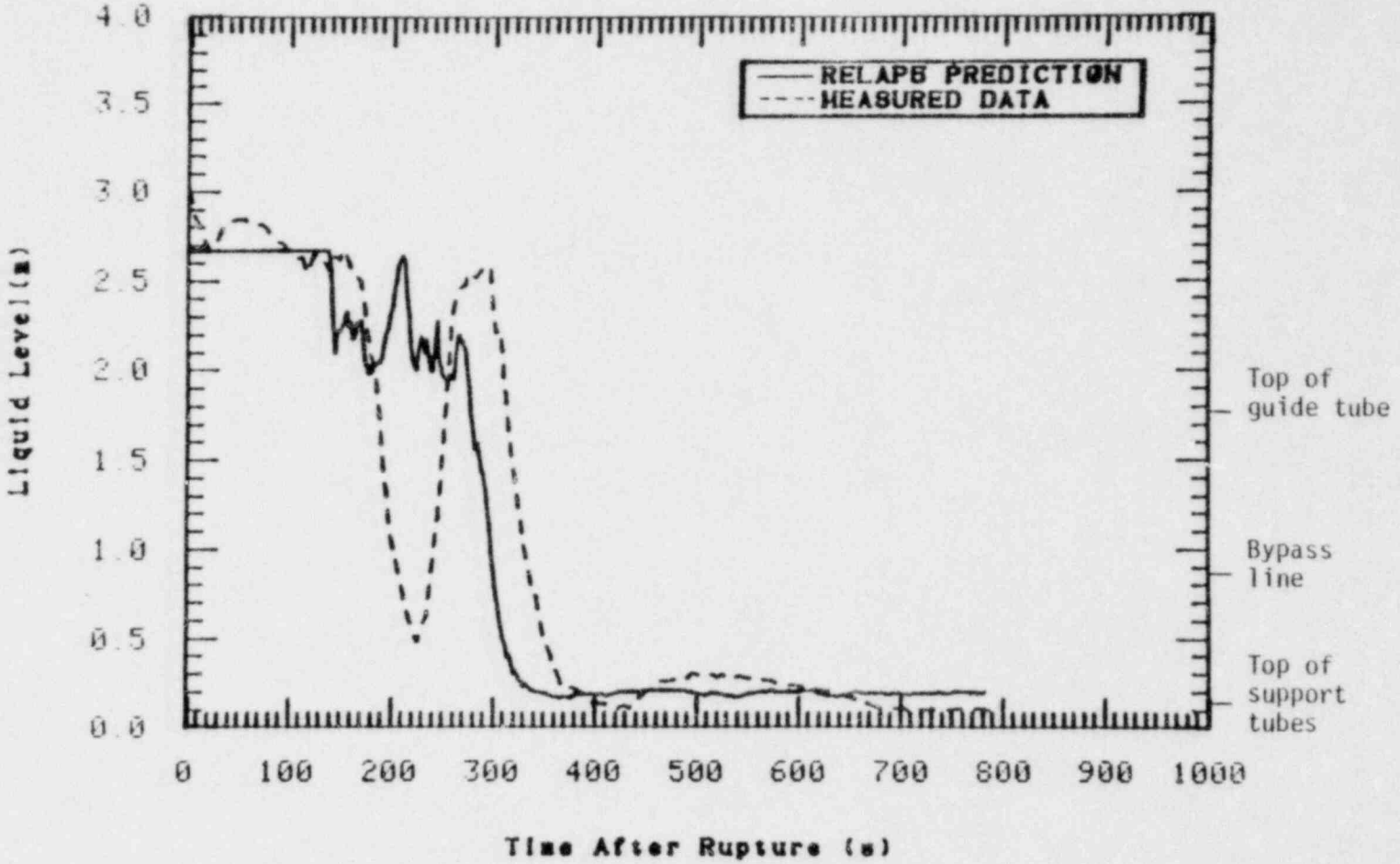

Figure 33. Comparison of calculated and measured upper head collapsed liquid level for Test S-UT-7.

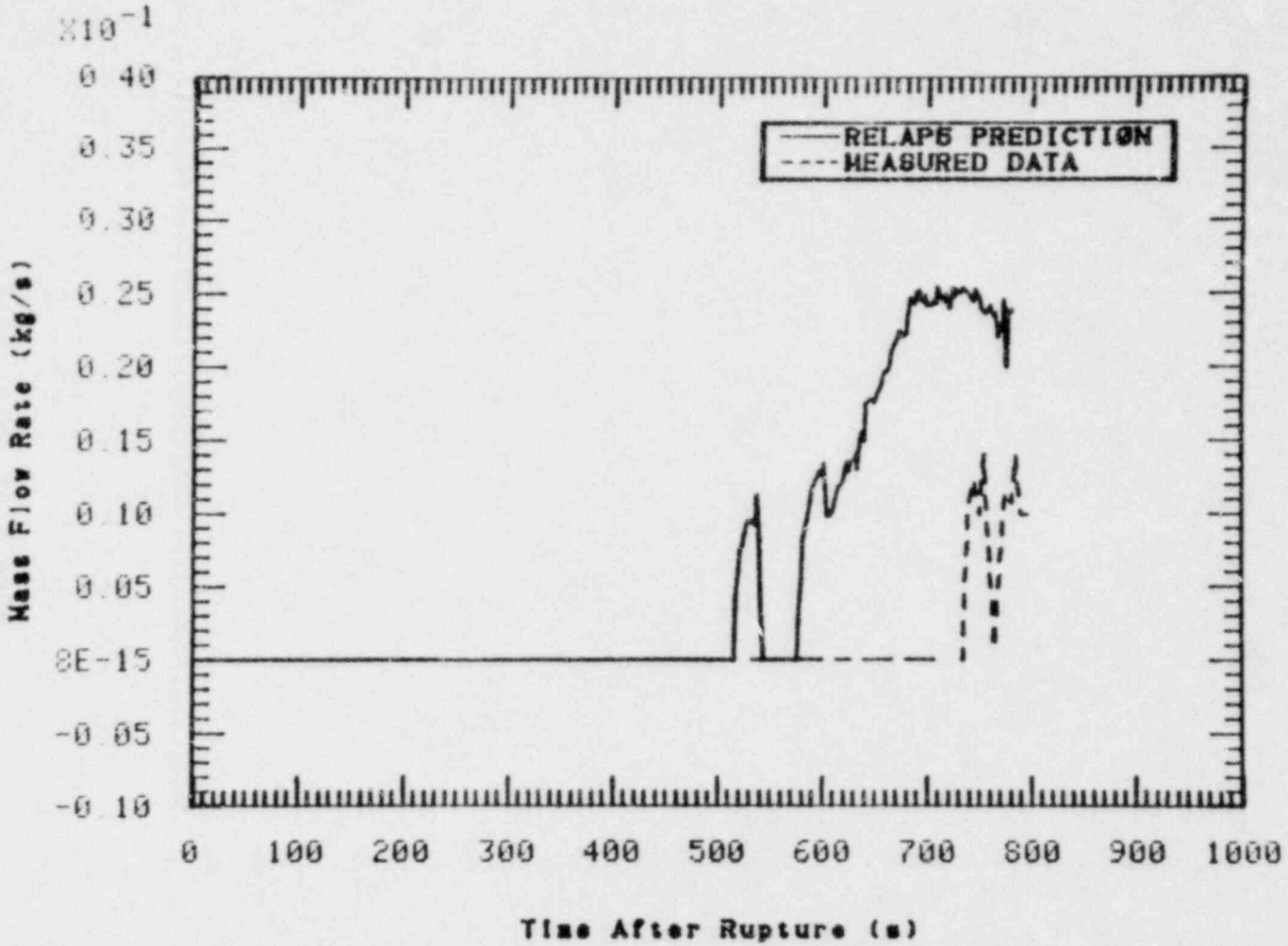

Figure 34. Comparison of calculated and measured broken loop accumulator flow rate for Test S-UT-7.

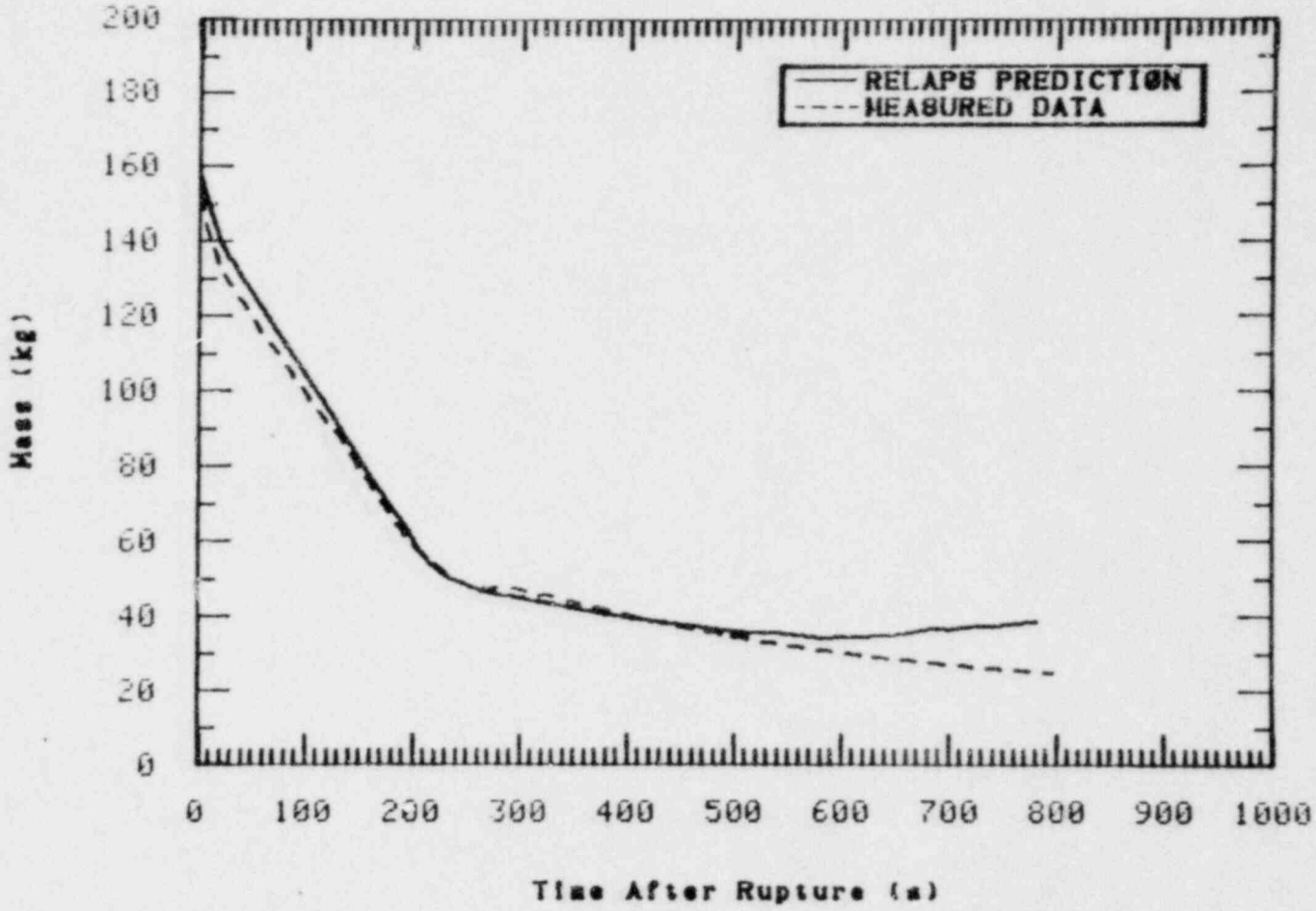

Figure 35. Comparison of calculated and measured system mass for Test S-UT-7.

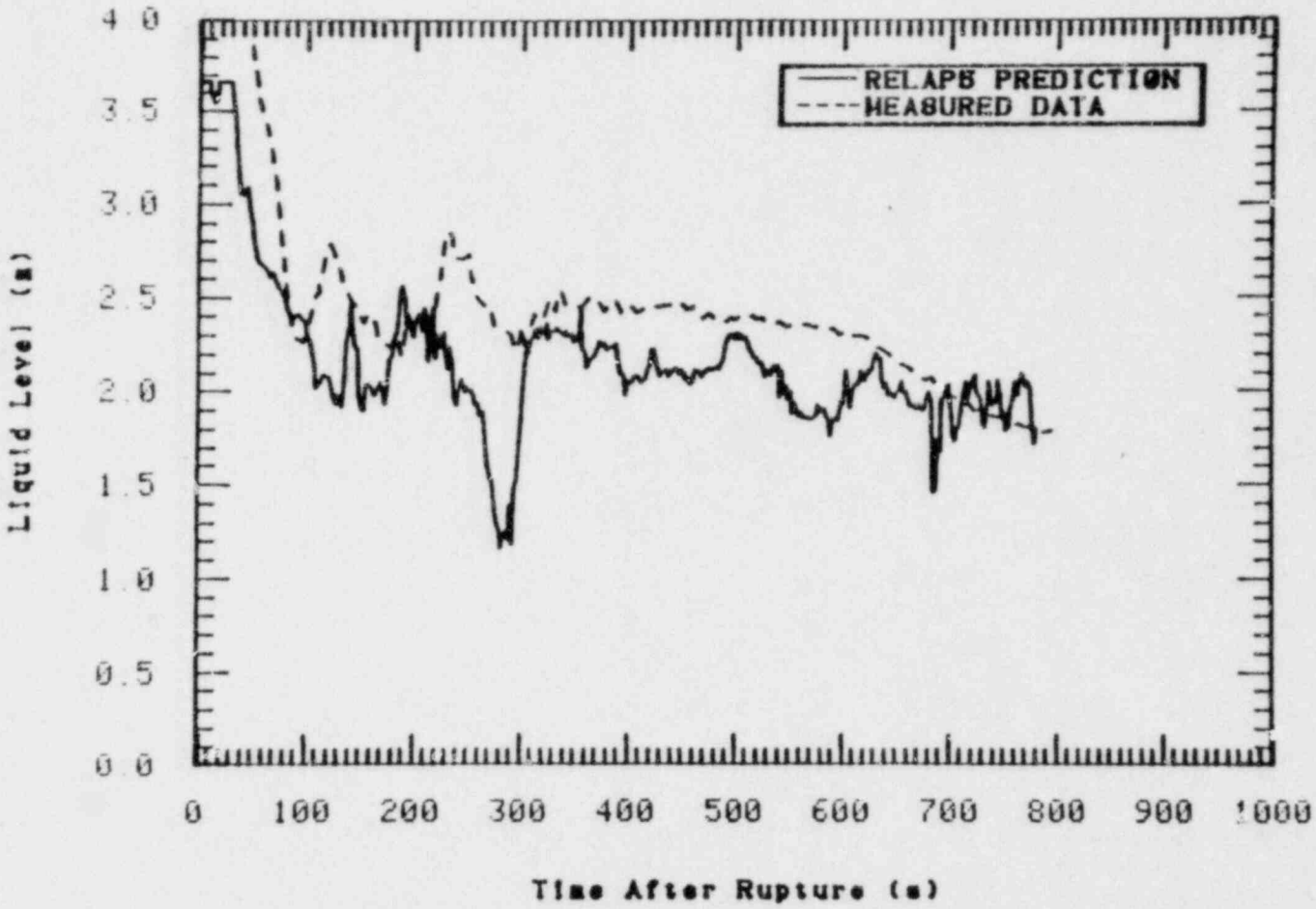

Figure 36. Comparison of calculated and measured core collapsed liquid level for Test S-UT-7.

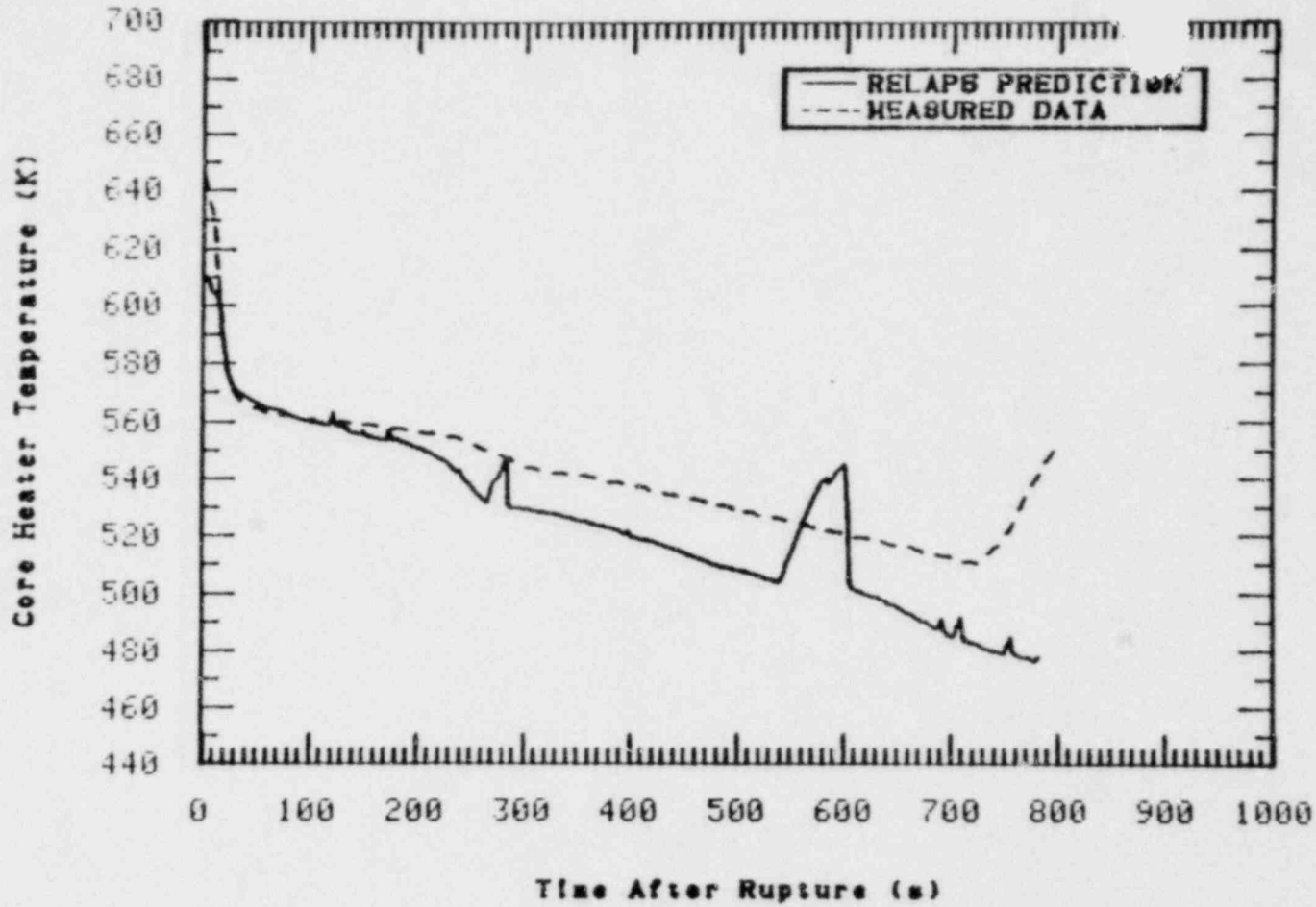

Figure 37. Comparison of highest calculated cladding temperature (305 - 335 cm elevation) and measured temperature THV*B4+322) for Test S-UT-7.

temperature is a surface temperature.) Temperature excursions did not occur in the experiment prior to 700 s because the higher liquid inventory in the core provided sufficient cooling of the heater rod.

The higher depressurization rate in the calculation resulted in earlier emptying of the upper head accumulator (Figure 38). Comparison of Figures 38 and 33 shows that in both the calculation and the experiment draining of the upper head began shortly after emptying of the upper head accumulator and took approximately 50 s. During the draining process liquid flowed out of the upper head through the bypass line and support columns while vapor flowed into the upper head through the guide tube. Figures 39 and 40 show that this was the draining mechanism in both the calculation and the experiment although the magnitudes of the calculated upper head flows are somewhat different than the measured values.

Comparison of the S-UT-7 pretest calculation with the S-UT-6 pretest calculation (Reference 5) shows that, with UHI, the calculated core liquid depletion (Figure 41) and corresponding heatup (Figure 42) are of smaller magnitude. Thus, the calculated effects of UHI on the core behavior were a reduction of liquid depletion and heatup. Figure 23, however, shows that the magnitude of these effects was overcalculated. The apparent reason for the overcalculation of the effects of UHI was that the calculated vapor velocity was too high at the break as discussed previously. As a result of the high vapor velocity, the calculated break volumetric flow was also too large which resulted in too much vapor generation in the vessel. Without the addition of liquid from the UHI system (Test S-UT-6) the vapor generation in the vessel caused extensive liquid depletion and heatup in the core as shown in Figures 41 and 42.

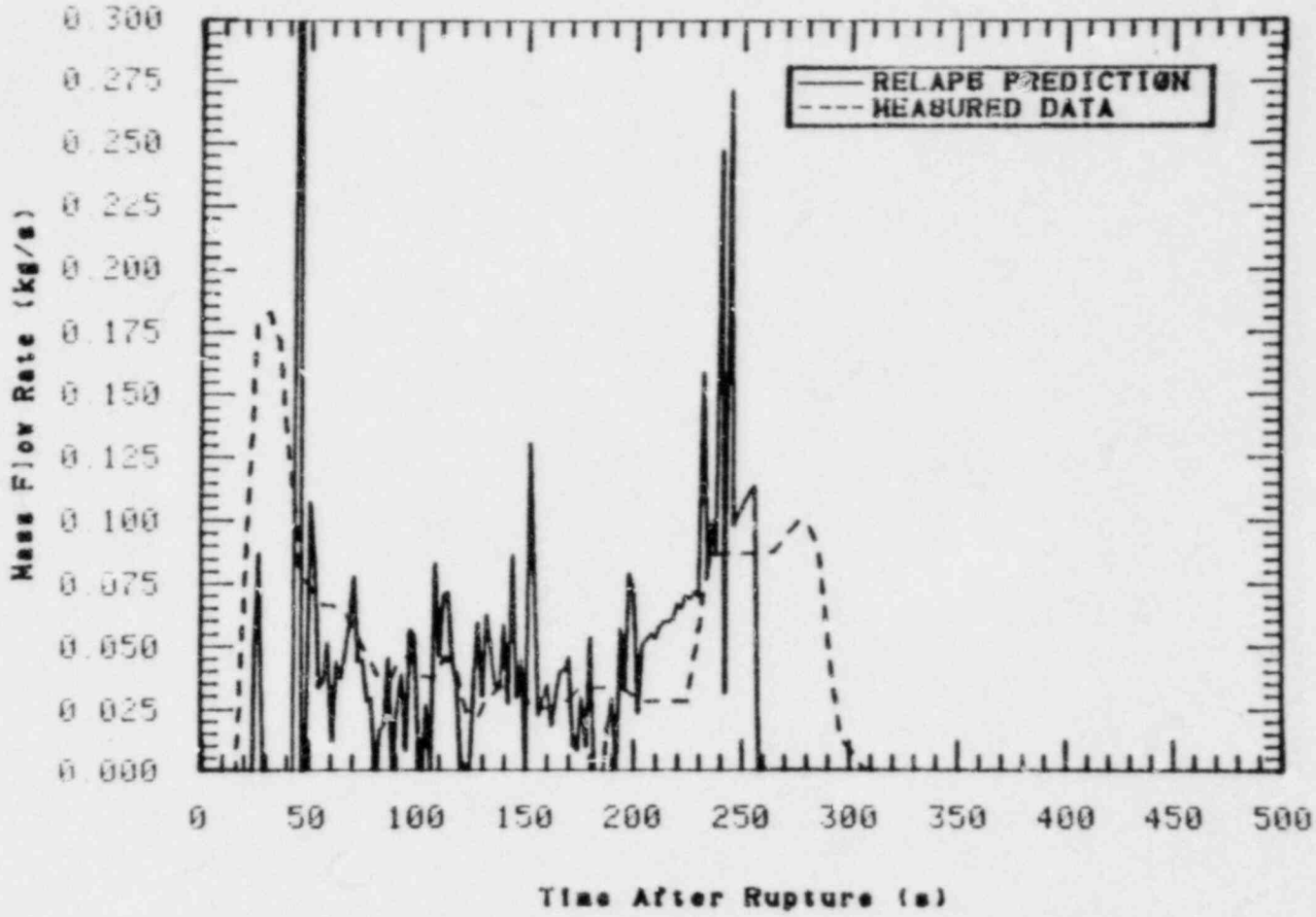

Figure 38. Comparison of calculated and measured upper head accumulator flow rate for Test S-UT-7.

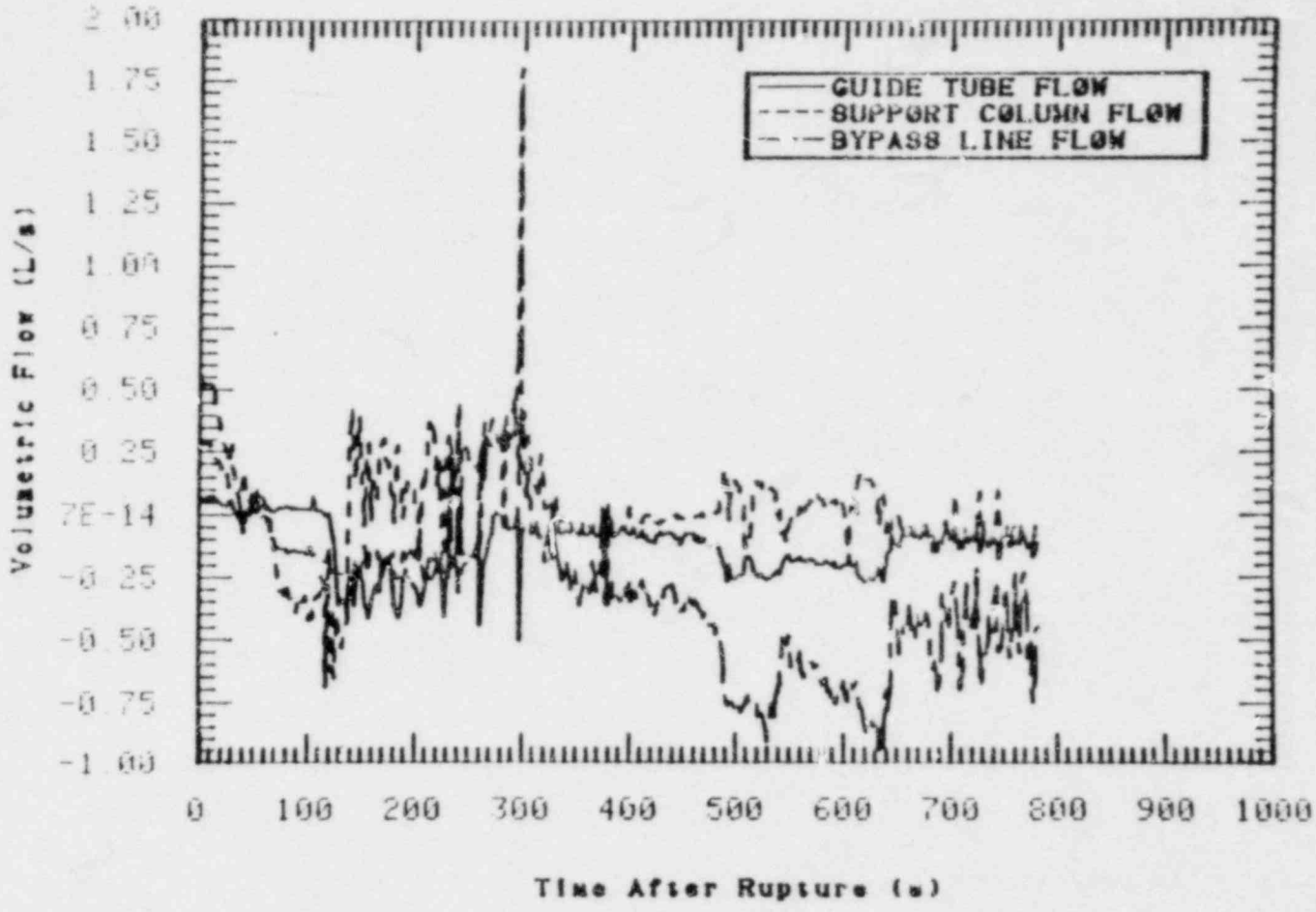

Figure 39. Calculated upper head volumetric flow for Test S-UT-7.

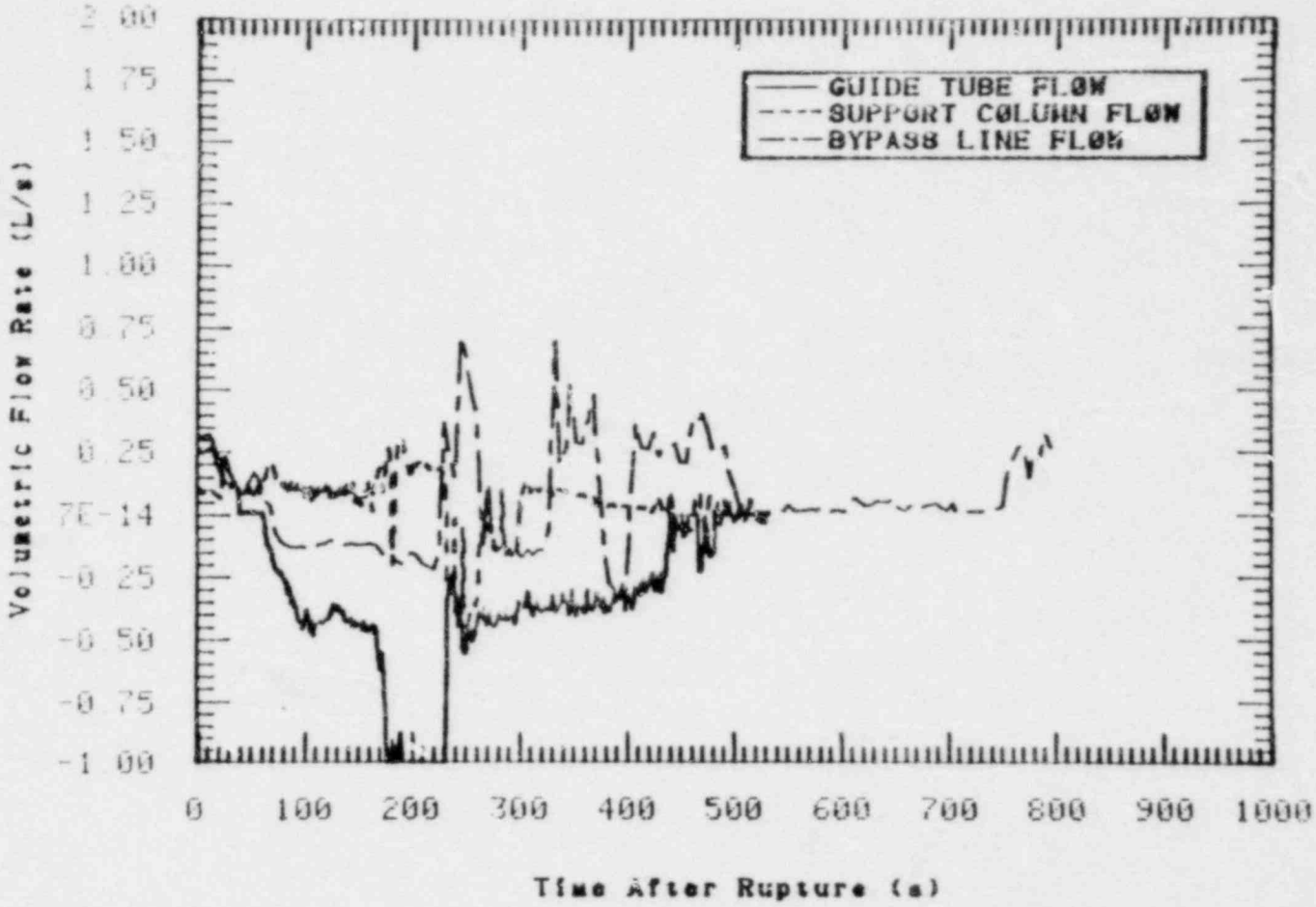

Figure 40. Measured upper head volumetric flows for Test S-UT-7.

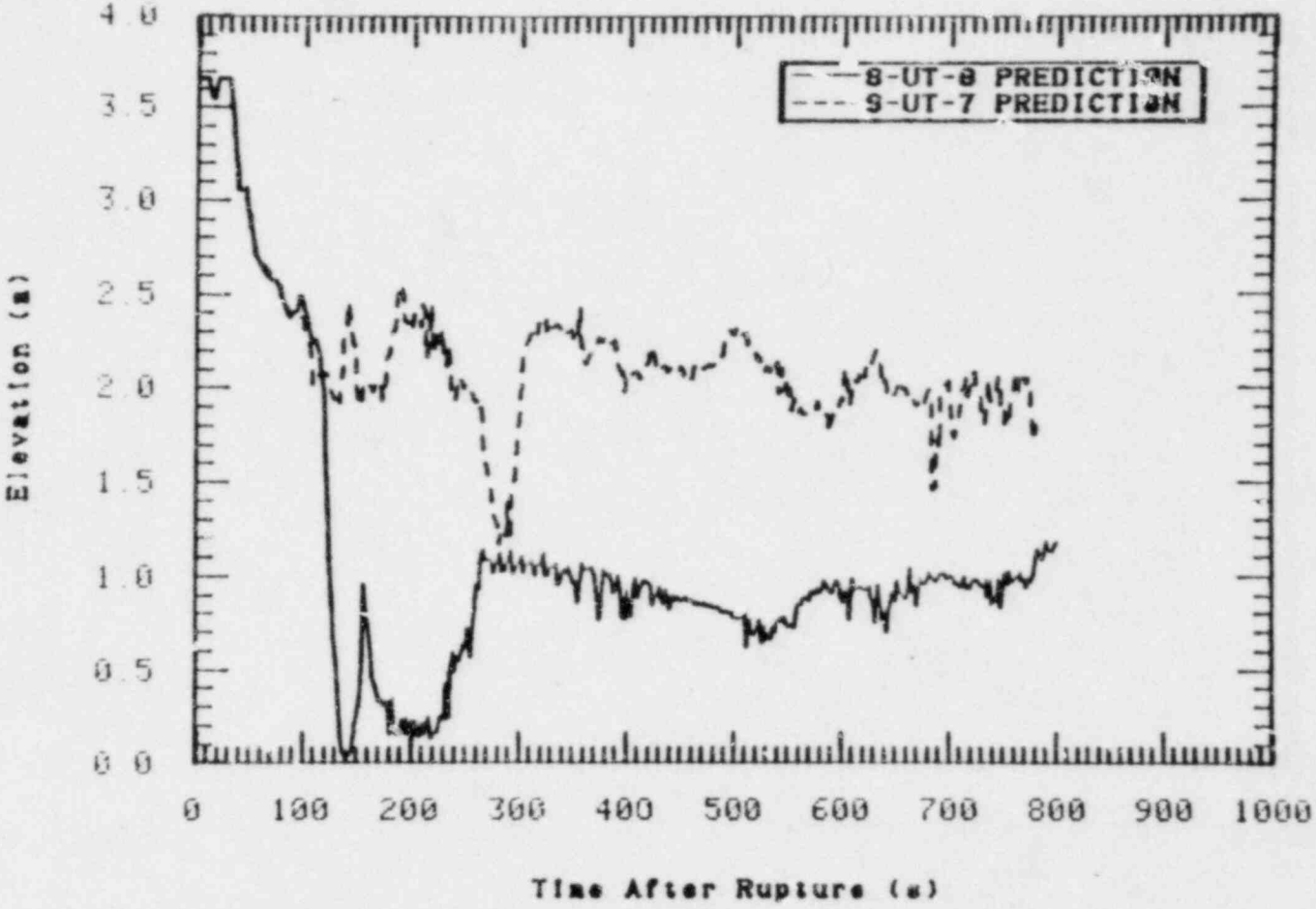

Figure 41. Comparison of calculated core collapsed liquid level for Tests S-UT-8 and S-UT-7.

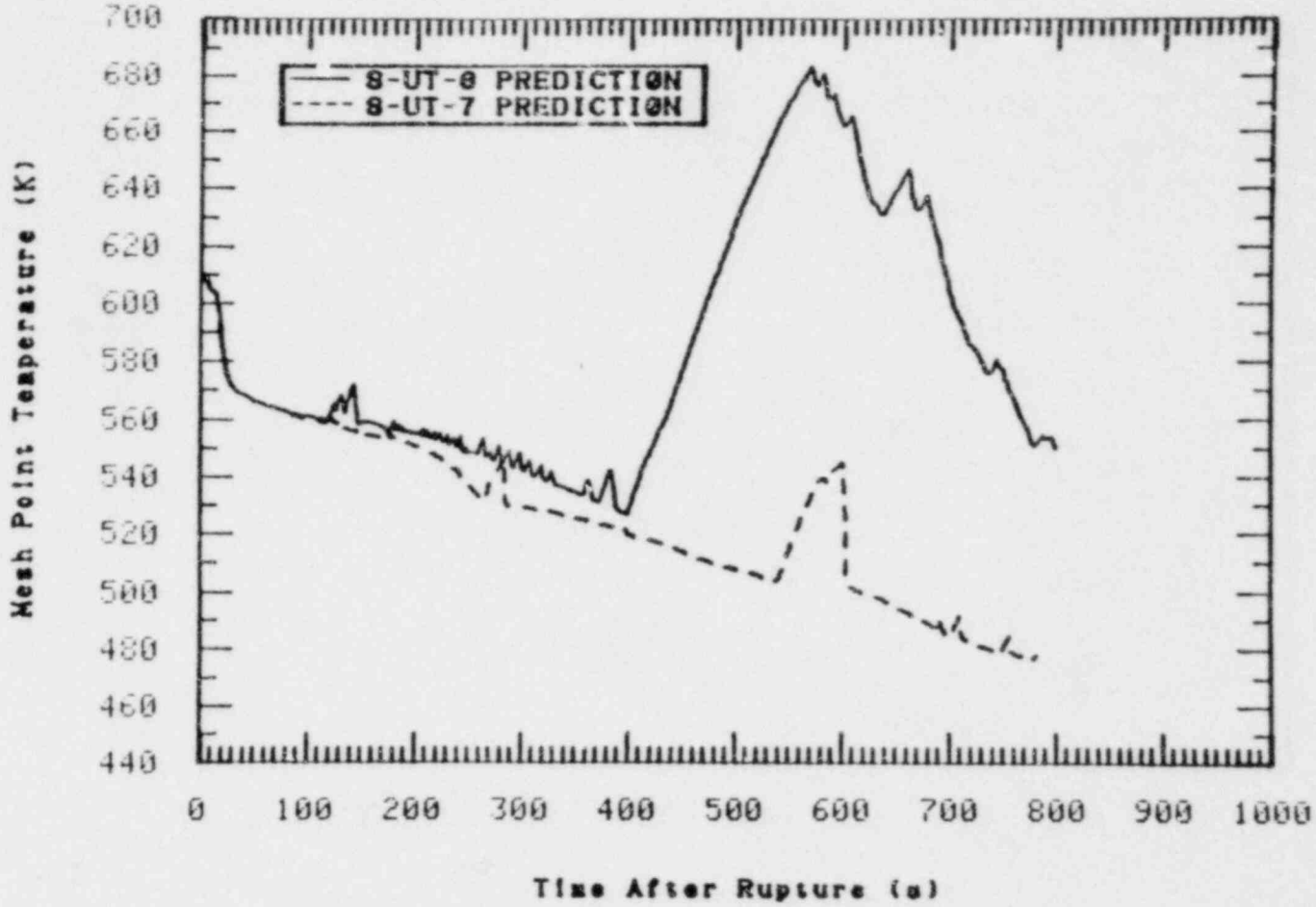

Figure 42. Comparison of calculated 305-335 cm elevation cladding temperature for Tests S-UT-6 and S-UT-7.

5. CONCLUSIONS

Results from Test S-UT-7 have provided information about system pressure response, fluid mass distribution, core coolability, and ECC injection effects for a 5% communicative, cold leg break, loss-of-coolant experiment with upper head and cold leg ECC injection. The test met its objective of providing thermal-hydraulic data to be used in assessing computer code performance and for evaluating the relative effects of upper head injection during a small break LOCA.

Injection of UHI fluid during a 5% cold leg break experiment provided sufficient mass addition to the core inventory so as to reduce the degree of core heatup by 100 K. The UHI liquid was found to pass both to the break and to the core region.

Results of the RELAP5 pretest prediction compared reasonably well with test data. Posttest analysis will be required to fully account for deficiencies in the calculation.

6. REFERENCES

1. T. K. Larson, J. L. Anderson, and D. J. Snimeck, Scaling Criteria and An Assessment of Semiscale Mod-3 Scaling for Small Break Loss-of-Coolant Transients, EGG-SEMI-5121, EG&G Idano, Inc. Marcn 1980.

2. P. Northn, ltr to R. E. Tiller, Experiment Operating Specification (EOS) for Semiscale Mod-2A 5% Break Experiments, Tests S-UT-6 and S-UT-7, PN-58-81, EGG-SEMI-5421, EG&G Idano, Inc., April 1981.

3. System Design Description for the Mod-3 Semiscale System (Revision B), EG&G Idano, Inc., December 1980.

4. P. Northn ltr to R. E. Tiller, Test Prediction for Semiscale Mod-2A Small Break Test S-UT-7, PN-41-81, EG&G Idano, Inc., April 21, 1981.

5. P. Northn ltr to R. E. Tiller, Test Prediction for Semiscale Mod-2A Small Break Test S-UT-6, PN-40-81, EG&G Idano, Inc., April 14, 1981.

APPENDIX A

APPENDIX A

The pretest calculation for Semiscale Test S-UT-7[a] was performed using RELAP5/MOD1 (released version 6).[b] A model nodalization diagram used for the calculation is shown in Figure A-1. The model consists of 175 hydrodynamic volumes and 197 heat structures. All volume parameters are calculated with nonequilibrium code models. Break flow multipliers of 0.80 and 0.90 are used for subcooled and two-phase discharge coefficients, respectively. Information gained from the heat loss characterization tests concerning the magnitude and distribution of system heat losses was incorporated into the model. System guard heaters are powered to offset environmental system heat losses.

---

a. Historical code configuration control number F00227.

b. Historical code configuration control number F00181.

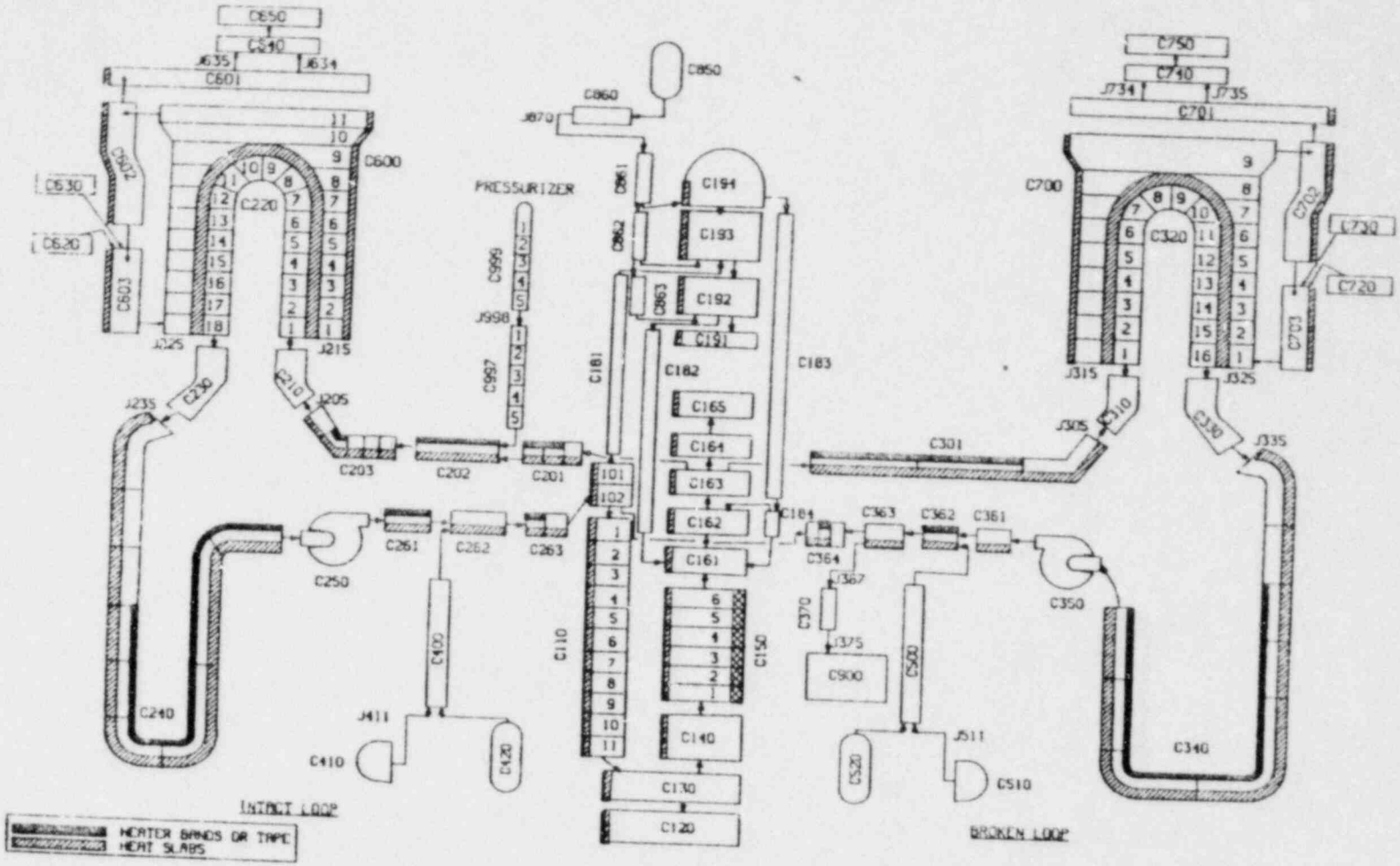

Figure A-1. RELAP5 nodalization diagram for the Semiscale Mod-2A system.